diversity

MDPI

Article

Variation in the Jaw Musculature of Ratsnakes and Their Allies (Serpentes: Colubridae)

Bartosz Borczyk [1,*] and Tomasz Skawiński [2]

[1] Department of Evolutionary Biology and Conservation of Vertebrates, Faculty of Biological Sciences, University of Wrocław, Sienkiewicza 21, 50-335 Wrocław, Poland
[2] Museum of Natural History, Faculty of Biological Sciences, University of Wrocław, Sienkiewicza 21, 50-335 Wrocław, Poland; tomasz.skawinski@uwr.edu.pl
* Correspondence: bartosz.borczyk@uwr.edu.pl

Abstract: Snakes have a highly modified feeding apparatus. However, its associated musculature is often poorly known. In order to study variation in the cephalic musculature, we dissected specimens representing 28 snake species belonging to the New World clade Lampropeltini and their Old World relatives. The observed variation was analysed using a phylogenetic framework. We found that the pattern of their musculature is conservative. We observed no interspecific variation in the intermandibular muscles or in the posterior jaw adductors. Variation within the dorsal constrictors and lateral jaw adductors is relatively low. This could be explained by morphological (space) limitations and functional constraints.

Keywords: anatomy; comparative morphology; evolution; myology; snakes

check for updates

Citation: Borczyk, B.; Skawiński, T. Variation in the Jaw Musculature of Ratsnakes and Their Allies (Serpentes: Colubridae). *Diversity* **2023**, *15*, 628. https://doi.org/10.3390/d15050628

Academic Editor: Adán Pérez-García

Received: 31 March 2023
Revised: 2 May 2023
Accepted: 3 May 2023
Published: 5 May 2023

1. Introduction

The snake suborder is a very specialised radiation of squamate reptiles that encompasses more than 4000 extant species [1]. They evolved a very particular feeding apparatus among tetrapods [2–6]. Although their skull diversity is well studied (see [7] for a review), data on their jaw musculature are restricted to relatively few groups, the papers are usually descriptive, and comparisons deal with only distantly related taxa (e.g., [8–17]). Although significant progress has been made toward resolving the homology of jaw adductors and inter-family variation [17–20], little is known about variation at a lower level; only a small fraction of such studies have focused on closely related species [21–24].

The snakes described in a recent paper belong to a radiation of New World Lampropeltini (genera studied here: *Lampropeltis* and *Pantherophis*) and their Old World relatives, represented by *Coronella*, *Elaphe*, *Euprepiophis*, *Gonyosoma*, *Oreocryptophis*, *Orthriophis*, *Zamenis*, and *Coelognathus* [25–29] (Figure 1). These species live in a wide variety of habitats, from wet tropical forests to semiarid areas, and they can be arboreal or semiarboreal and ground dwelling or burrowing species that feed on small vertebrates (mostly mammals and birds; see [30,31]).

The jaw musculature of Lampropeltini has only been seriously studied by Albright and Nelson [9], who studied *Pantherophis obsoletus*; however, their studies were rather general and oriented towards the subsequent analysis of functional morphology [32]. Earlier studies by Radovanović [33] dealt with *Elaphe quatuorlineata*, *Zamenis longissimus*, *Z. situla*, and dozens of distantly related species, but his descriptions were very general and erroneous in some details (see Section 4).

In this paper, variation within the cephalic muscles of 28 species, representing 10 genera of New and Old World ratsnakes and their closest allies, is presented.

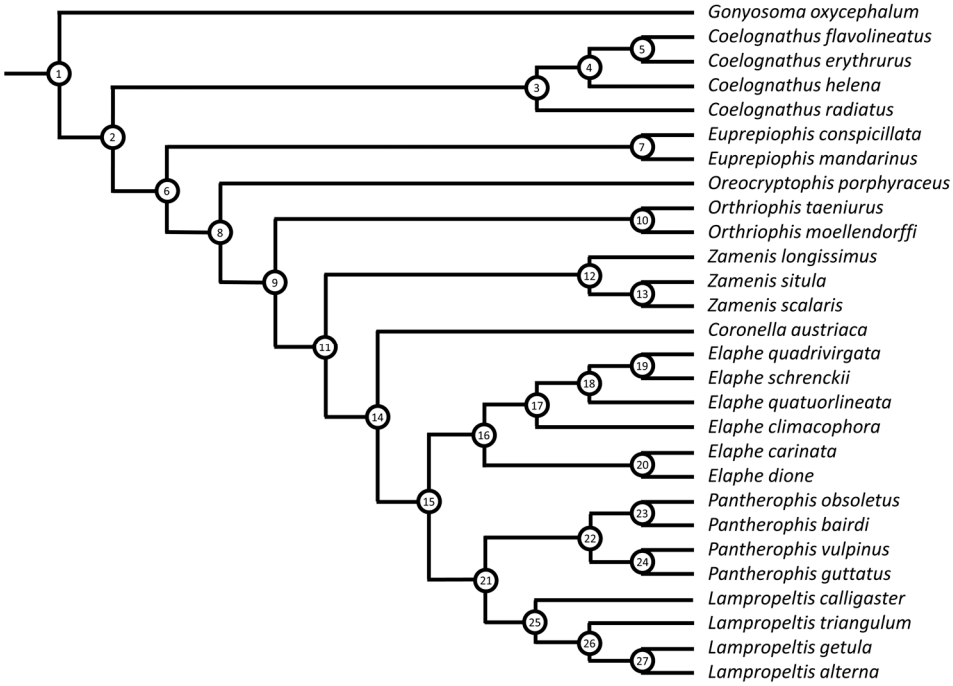

Figure 1. Phylogenetic hypothesis of the studied species adopted in this work. It follows Zaher et al. [29], except for in the interrelationships within *Elaphe*, which follow TimeTree [34]. Numbers in the nodes refer to Table S1.

2. Materials and Methods

The specimens examined were *Coelognathus helena* (IZK 411–413); *Coe. radiatus* (MNHW four unnumbered specimens, ZMB 42855); *Coe. flavolineatus* (ZMB 47936); *Coe. erythrurus* (FMNH 53435); *Gonyosoma oxycephalum* (IZK 331–333, 337, 405, MNHW unnumbered specimen); *Euprepiophis conspicillata* (BB 048, ZMB 26568); *Euprepiophis mandarinus* (FMNH 223968, IZK 407, ZFMK 5219); *Oreocryptophis porphyraceus* (FMNH 24913, ZMB 48053); *Orthriophis taeniurus* (BB 004, 013, 014, 032, 042, 043, IZK 365, 366, 410); *Orthriophis moellendroffi* (IZK 414–416, MNHN 1990.4316); *Elaphe dione* (MNHW four unnumbered specimens, ZMB 31427); *Elaphe carinata* (FMNH 24906, ZMB 47837), *Elaphe climacophora* (ZMB 26502), *Elaphe quadrivirgata* (BB 045–047, ZMB 66114), *Elaphe quatuorlineata* (ZFMK 5017, 5218, ZMB 63769); *Elaphe schrenckii* (IZK 406); *Zamenis scalaris* (ZMB 36138); *Zamenis longissimus* (IZK 338, 364, MNHW unnumbered specimen); *Zamenis situla* (IZK 384, MNHW seven unnumbered specimens); *Coronella austriaca* (BB 040, IZK 400-403); *Pantherophis guttatus* (BB 005, 006, 015, 016, 044); *Pantherophis bairdi* (IZK 393); *Pantherophis obsoletus* (IZK 387–390, ZMB 58453); *Pantherophis vulpinus* (FMNH 22341); *Lampropeltis getula* (BB 002, 008, 041, IZK 395, 386); *Lampropeltis alterna* (IZK 409); and *Lampropeltis calligaster* (FMNH 8475, IZK 391).

The snakes' heads were dissected using a NIKON SMZ-U binocular equipped with a camera lucida. To better define the direction of the muscle fibres, Lugol's iodine staining was used [35].

The description used *Elaphe schrenckii* as a model, followed by remarks on the variation in other studied species (if any). The terminology used for the ventral constrictor and intermandibular muscles followed that of Cundall [24]. The terminology used for the jaw adductors followed that of Johnston [19] and Das and Pramanick [17], however the terminology for external adductors is still under debate (e.g., [16,18,19,36]). The osteological terminology used follows Cundall and Irish [7].

Phylogenetic Framework and Statistical Analyses

In this article, we use the name Colubridae in the broad sense, i.e., as encompassing, for example, Colubrinae, Natricinae, and Xenodontinae (e.g., [1]). However, it is worth

noting that these taxa are considered separate families of colubroid snakes by some other authors (e.g., [27,29]).

The phylogenetic hypothesis of the analysed species follows Zaher et al. [29], except for in the interrelationships within *Elaphe*, which follow TimeTree [34] (Figure 1). The branch lengths were adjusted according to the estimated divergence dates between taxa (mostly after TimeTree [34]; see exact values in Table S1). The resulting phylogenetic tree was then analysed in R 4.2.2 [37] and the add-on package ape 5.0 [38]. To estimate the phylogenetic signal in analysed characters, we calculated the δ parameter [39]. In brief, high values of δ indicate strong phylogenetic signal, i.e., that closely related species are more similar to one another than to species drawn randomly from the same tree. *Coelognathus flavolineatus* is polymorphic in one of the characters (M6), so the phylogenetic signal in that character was calculated in two iterations—first, with *C. flavolineatus* scored as 0, and second, scored as 1.

Ancestral state reconstructions were conducted in Mesquite 3.61 [40] using Maximum Likelihood ('current probability models').

3. Results

3.1. Phylogenetic Signal and Ancestral State Reconstructions

Of the fourteen analysed characters, five showed a statistically significant phylogenetic signal. The values of the δ parameter for these characters are between 2.239 and 12.280 (Table 1). For two characters (M9 and M10), it was not possible to calculate the *p*-value, but relatively low values of the δ parameter (1.85 and 1.27, respectively) suggest a weak phylogenetic signal at best.

Ancestral states were successfully reconstructed for thirteen characters (see below); it was not possible to reconstruct the ancestral state of one character because it exhibited intraspecific polymorphism within *Coelognathus flavolineatus*. The exact proportional likelihood values for each character at each node are given in Supplementary File S1.

Table 1. Phylogenetic signal (δ parameter) calculated for the analysed myological characters. Characters showing a statistically significant phylogenetic signal are marked with a single asterisk. Two asterisks indicate an analysis in which *Coelognathus flavolineatus* was scored as 0 and three asterisks indicate an analysis in which it was scored as 1. M1—variation of levator anguli oris type of aponeurosis, M2—the levator anguli oris insertion type, M3—levator anguli oris origin, M4—Musculus adductor mandibulae externus superficialis division, M5—basal aponeurosis of Musculus adductor mandibulae externus medialis, M6—depressor mandibulae division, M7—Musculus pseudotemporalis origin, M8—levator pterygoidei insertion, M9—protractor pterygoidei insertion; M10—protractor pterygoidei origin, M11—retractor pterygoidei; insertion, M12—retractor pterygoidei origin, M13—retractor vomeris origin, M14—retractor vomeris aponeurosis.

Character	δ	*p*
M1 *	2.239	0.01
M2	0.327	0.4
M3 *	4.145	0.02
M4	12.280	0.01
M5 *	1.003	0.58
M6	0.8719 ** 1.380 ***	0.17 ** 0.08 ***
M7	0.2348	0.38
M8	0.7048	0.24
M9	1.850	-
M10	1.270	-
M11 *	2.626	0.03
M12	0.7748	0.05
M13	0.5753	0.1
M14 *	4.109	0.01

3.2. Jaw Adductor Complex

3.2.1. Levator Anguli Oris (LAO)

The LAO is the most rostral of the jaw adductors (Figure 2). It is a large muscle and is triangular in shape. It originates on the postorbital and parietal bones. The LAO is partially covered by the quadrate-maxillary ligament and upper labial gland. Near the mouth corner, it is also covered by the posterior part of the Harderian gland and the connective tissues of the mouth corner. The LAO covers the dorsal part of the Harderian gland and the deeper layers of the jaw adductors. Initially, its fibres pass caudo-ventrally and turn around the mouth corner in the antero-ventral direction. None of the fibres reach the mandible, but they make contact via a broad aponeurosis (type I sensu Borczyk [41]; see below and Figure 3), which inserts from approximately the distal half of the quadrate and compound bone and goes rostrally as far as the caudal end of the dentary. The mouth corner tissues and pad tightly cover the region, but no fibres were found inserting into them in this analysis.

This muscle shows the greatest variation in its jaw-insertion pattern. Its aponeurosis can be divided into three main types [41]: I—broad aponeurosis, inserting into approximately one half of the quadrate bone length and to the long portion of the compound bone; II—partly reduced aponeurosis, which only attaches onto part of the quadrate (approximately 1/4 of its distal length) and compound bone; and III—reduced aponeurosis, only inserting into the compound bone (Figure 4). In addition to its three different aponeurosis patterns, the LAO may insert into the lower jaw through the aponeurosis only or may contact the compound bone directly in addition to through the aponeurosis (Figures 3 and 5).

Cranial origin shapes and positions remain rather invariant; *Gonyosoma oxycephalum* is an exception, in which the insertion into the postorbital bone is very long (especially in young specimens) and almost reaches the ventral edge of the bone. In large *Gonyosoma* specimens, the LAO inserts into the postorbital bone for approximately one third of its length, suggesting interesting allometric patterns of muscle and bone growth. In the case of *Lampropeltis*, the insertion of the LAO is much shorter than in the other species, and, as such, seems to be a synapomorphy of this genus (Figure 6).

There is no subdivision of the LAO into two or more separate parts. The fibres that originate on the postorbital and parietal bones do not constitute separate parts and are indistinguishable through the whole muscle length; the only exception is *Coelognathus erythrurus* (FMNH 53435), in which, in the ventral part of the muscle, the part that inserts directly into the mandible is clearly separated from the rest of the muscle that inserts into the mandible via the aponeurosis. This division disappears at approximately the height of the quadrate-maxillary ligament. In the middle and dorsal part of the muscle, this subdivision is indistinguishable. In the case of species in which part of the LAO fibres insert into the mandible directly, the fibres originate from the postorbital bone, but there are always other fibres of the same origin that insert through the aponeurosis.

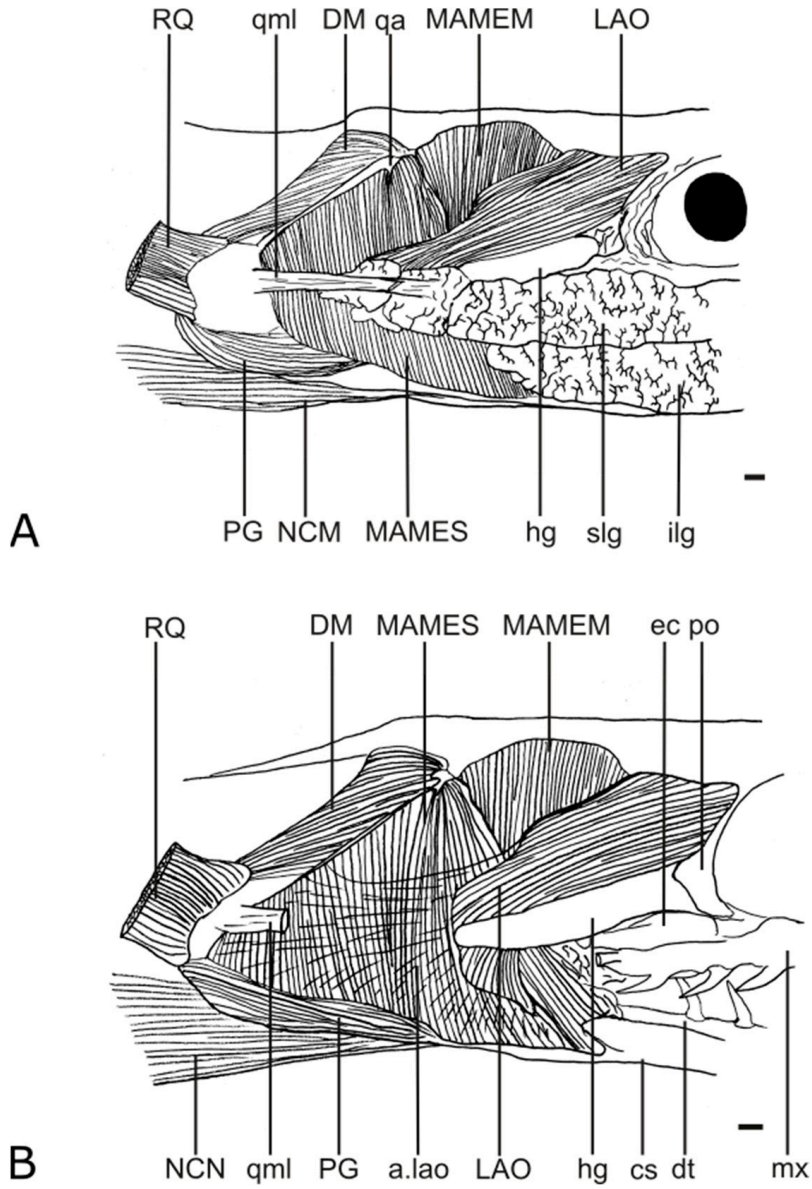

Figure 2. Lateral jaw musculature of *Elaphe schrenckii* (IZK 406). (**A**) skin removed, (**B**) glands and connective tissues removed. Note the wide (type I) aponeurosis of LAO.

In *Euprepiophis conspicillata*, *Elaphe carinata*, *El. climacophora*, *Coronella austriaca*, *Pantherophis guttatus*, and *P. vulpinus*, the part of the muscle that inserts directly into the mandible is very thin and often hardly distinguishable from the aponeurosis. In the case of *Coelognathus erythrurus* and *Oreocryptophis porphyraceus*, this part is very wide.

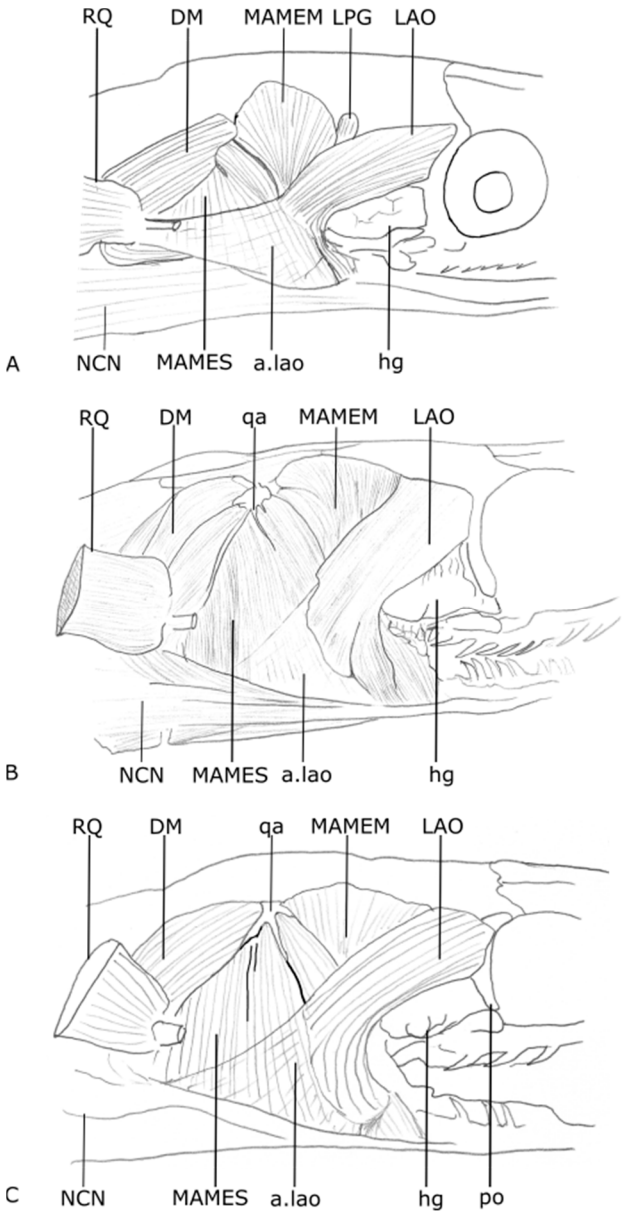

Figure 3. Partly reduced aponeurosis (type II) of levator anguli oris (LAO) in (**A**) *Euprepiophis conspicillata* (ZMB 2658) and strongly reduced aponeurosis in (**B**) *Coelognathus erythrurus* (FMNH 53435) and (**C**) *Lampropeltis triangulum* (IZK 409). The wide aponeurosis of LAO (type I) is shown in Figure 2B.

Orthriophis are characterised by a relatively short LAO; their longest fibres only reach the quadrate-maxillary ligament, and further contact with the lower jaw is maintained through a wide (type I) aponeurosis. In the other species in which the LAO has no direct contact with the mandible (*El. schrenckii*, *El. quadrivirgata*, *El. dione*, *Coe. flavolineatus*, *Eu. mandarinus*, *G. oxycephalum*, *P. bairdi*, *Z. situla* and all *Lampropeltis*), this muscle is relatively long, separated from the lower jaw only by a thin strip of aponeurosis. In some cases, being able to properly recognise whether the muscle inserts into the mandible directly or via an aponeurosis may pose a problem.

A broad, type I aponeurosis is characteristic of *Elaphe carinata*, *El. climacophora*, *El. schrenckii*, *El. quadrivirgata*, *Euprepiophis mandarinus*, *Orthriophis taeniurus*, and *Ort. moellendorffi*. Type II aponeuroses characterise *Elaphe dione*, *El. quatuorlineata*, *Euprepiophis conspicillata*, and *Coronella austriaca*. The greatest reduction in aponeuroses may be observed in *Coelognathus erythrurus*, *Coe. flavolineatus*, *Gonyosoma oxycephalum*, *Oreocryptophis porphyraceus*, *Pantherophis bairdi*, *P. guttatus*, *P. vulpinus*, *Zamenis scalaris*, *Z. situla*, *Lampropeltis getula*, *L. calligaster*, *L. alterna*, and *L. triangulum*.

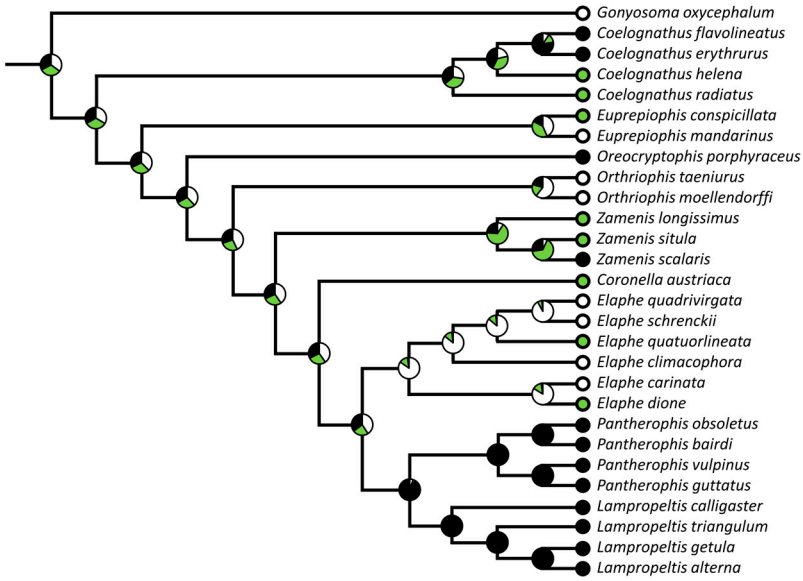

Figure 4. Variation in character states and reconstructed ancestral states of M. Levator anguli oris (LAO) (M1); type I aponeurosis (white), type II aponeurosis (green), type III aponeurosis (black). Proportional likelihoods for ancestral states are given in Supplementary File S1.

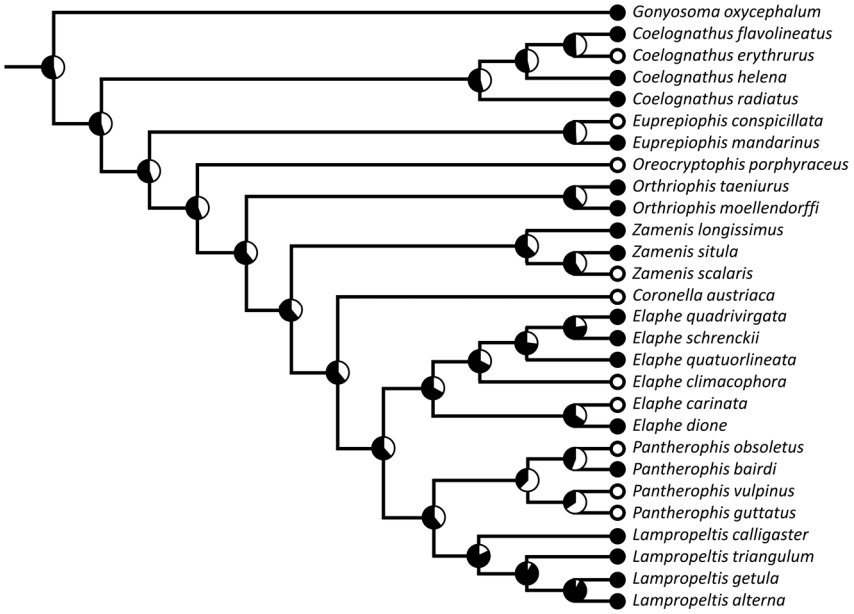

Figure 5. Variation in character states and reconstructed ancestral states of M. Levator anguli oris (LAO) (M2); the muscle contacts the mandible directly (white), or through an aponeurosis (black). Proportional likelihoods for ancestral states are given in Supplementary File S1.

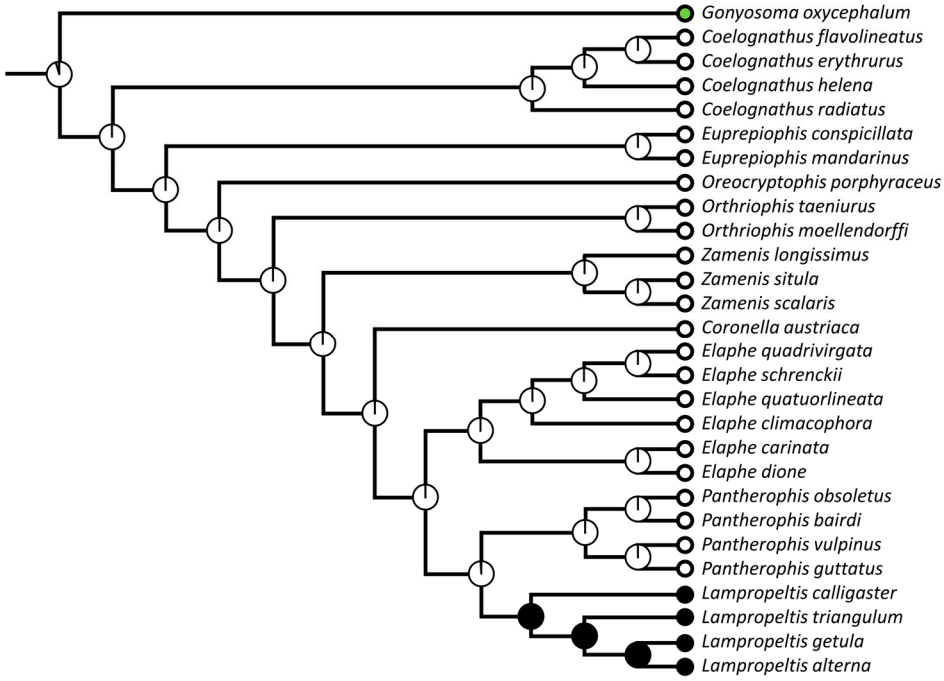

Figure 6. Variation in character states and reconstructed ancestral states of M. Levator anguli oris (LAO) (M3); insertion into the postorbital is of medium (white), long (green), or short (black) length. Proportional likelihoods for ancestral states are given in Supplementary File S1.

3.2.2. Musculus Adductor Mandibulae Externus Superficialis (MAMES)

The MAMES is the most posterior and biggest of the three external adductors (Figure 7). It is covered by the quadrate-maxillary ligament, upper and lower labial glands, and the LAO with its aponeurosis. It originates on the quadrate bone and quadrate aponeurosis, almost down to the jaw articulation. It inserts into the lateral part of the compound bone along the fossa mandibularis and rostrally reaches as far as the caudal end of the dentary. It also reaches the lateral edge of the dentary via connective tissues. The quadrate aponeurosis divides the MAMES into two parts; however, this division becomes undetectable in the ventral part of the muscle.

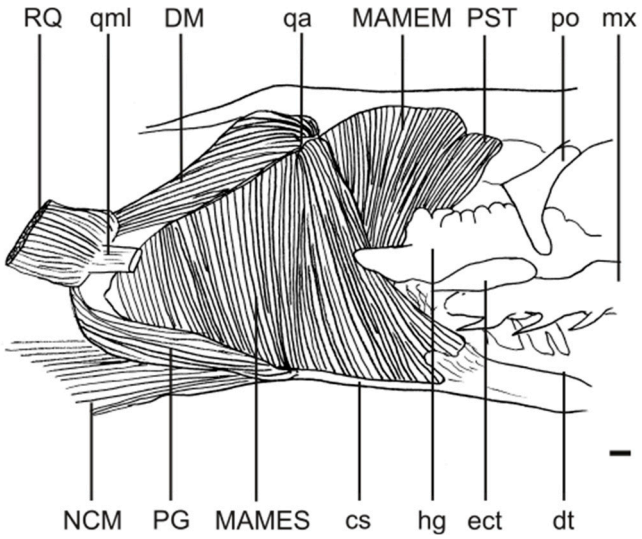

Figure 7. Jaw musculature of *Elaphe schrenckii* after removing M. levator anguli oris (LAO) and its aponeurosis. Note the anterior portion of MAMES reaches the lateral edge of the dentary via connective tissue.

Patterns of the subdivision of the MAMES by the quadrate aponeurosis are very variable (Figure 8). It may be undivided (*Pantherophis bairdi*, *P. guttatus*, *Gonyosoma oxycephalum*, *Elaphe quadrivirgata*, *El. quatuorlineata*, *El. carinata*, *Orthriophis moellendorffi*) or divided into two parts (*Lampropeltis getula*, *L. alterna*, *Pantherophis vulpinus*, *Coelognathus erythrurus*, *Coe. radiatus*, *Coe. flavolineatus*, *Oreocryptophis porphyraceus*, *Orthriophis taeniurus*, *Coronella austriaca*, *Elaphe climacophora*, *El. schrenckii*, *El. dione*, *Zamenis scalaris*, and *Z. situla*) or three parts (*Lampropeltis alterna*, *L. calligaster*, *Euprepiophis mandarinus*, *Eu. conspicillata*). Divisions, where present, are confined to the dorsal part of the muscle and disappear ventrally.

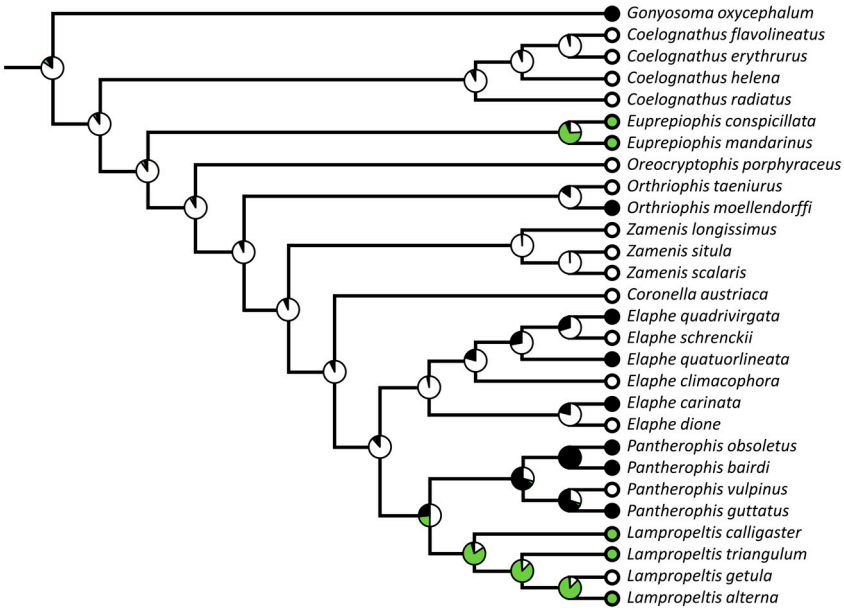

Figure 8. Variation in character states and reconstructed ancestral states of M. adductor mandibulae externus superficialis (MAMES) (M4); the muscle is divided by the quadrate aponeurosis into two bundles (white), three strands (green), or is undivided (black). Proportional likelihoods for ancestral states are given in Supplementary File S1.

3.2.3. Musculus Adductor Mandibulae Externus Medialis (MAMEM)

In the studied species, this muscle originates on the parietal bone through the middle and caudal part of the crista parietalis, on the supraoccipital bone (to the crista occipitalis) through the dorsal part of the ligament linking the supratemporal to the cranium, and on the supratemporal bone to the proximal part of the quadrate (Figures 9 and 10). It passes ventrally and is 180° twisted: its more superficial fibres turn antero-ventral, whereas the deeper fibres turn caudally in the ventral part of the muscle. In its rostral part, the MAMEM inserts into the compound bone via a short, largely reduced aponeurosis, whereas, caudally, this aponeurosis is absent.

In all of the studied species, except *Coelognathus erythrurus*, the MAMEM does not subdivide into separate parts. In this species, there is a visible, thin posterior part that originates from the supraoccipital and supratemporal bones and a wide anterior part that originates from the supraoccipital, supratemporal, and parietal bones.

The basal aponeurosis of the MAMEM inserts into the mandible and is clearly visible in all of the studied species, although it is usually reduced to a thin, triangular tendon in the rostral part of the insertion. The exception is *Euprepiophis mandarinus*; in this species, the aponeurosis is in the caudal part of the insertion. The degree of reduction in the basal aponeurosis differs between species and ontogenetically differs within species. In young specimens, it is much better developed in comparison to those in older ones. In adult specimens, the basal aponeurosis only remains strongly developed in two species: *Pantherophis bairdi* and *P. vulpinus*.

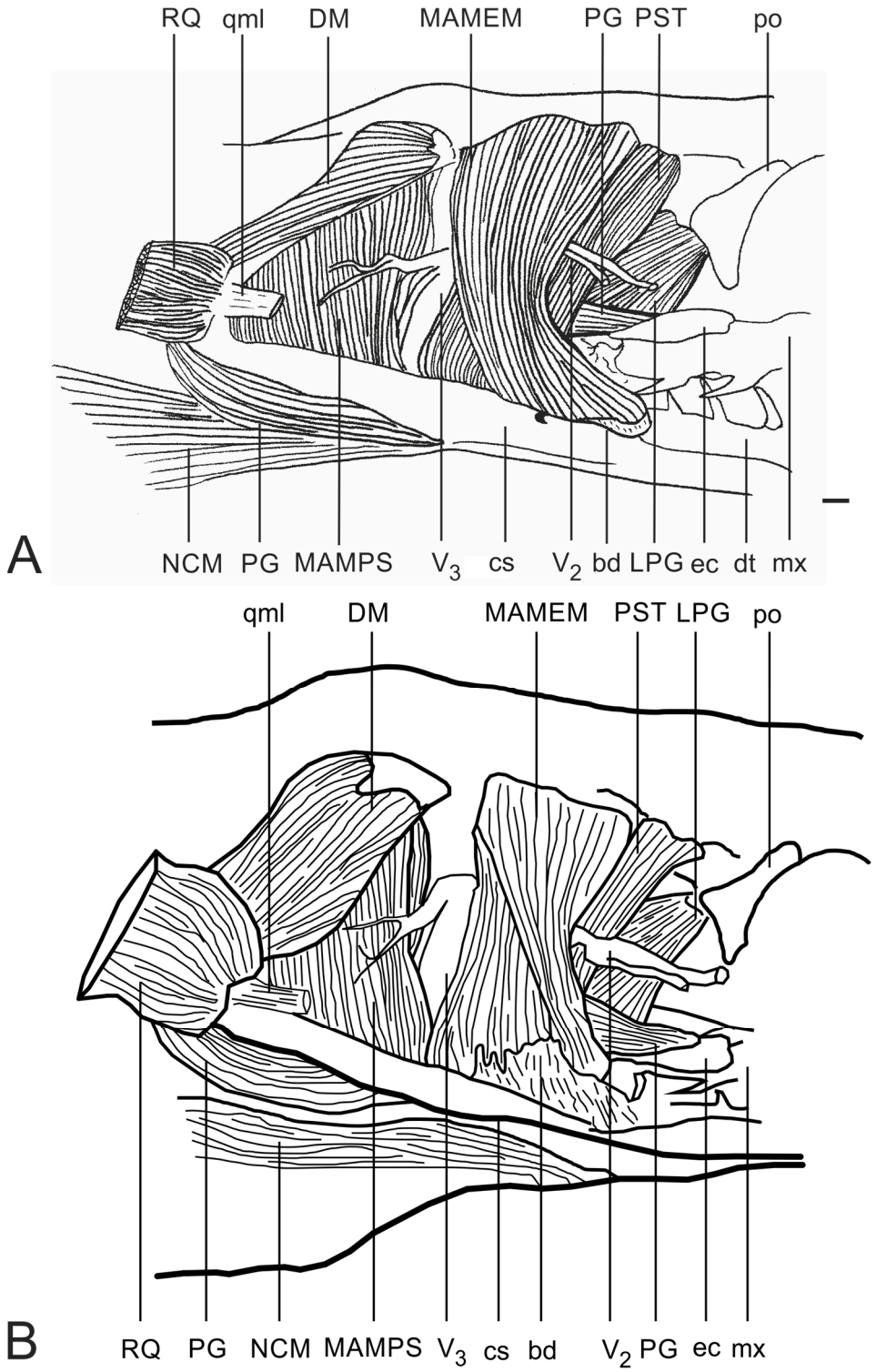

Figure 9. Jaw musculature after removing M. adductor mandibulae externus superficialis (MAMES) and Harderian gland (hg). (**A**) *Elaphe schrenckii*, (**B**) *Pantherophis vulpinus*.

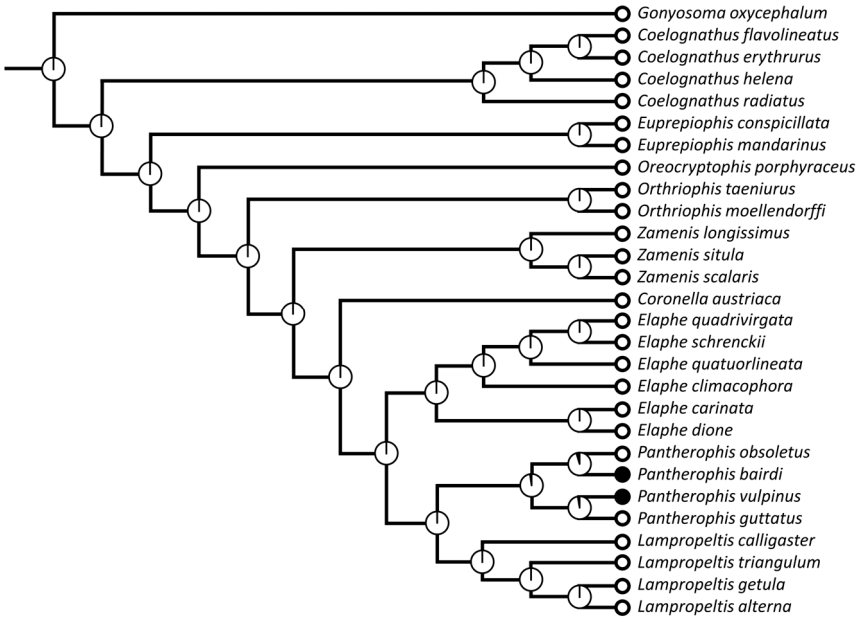

Figure 10. Variation in character states and reconstructed ancestral states of M. adductor mandibulae externus medialis (MAMEM) (M5); basal aponeurosis that is poorly developed (white), basal aponeurosis that is well-developed (black). Proportional likelihoods for ancestral states are given in Supplementary File S1.

3.2.4. Musculus Adductor Mandibulae Posterior Superficialis (MAMPS)

The MAMPS is a small muscle that originates from the anterior surface of the quadrate crest and ventrally inserts into the mandibular fossa, caudal to the mandibular branch of the trigeminal nerve (Figure 9).

3.2.5. Musculus Adductor Mandibulae Posterior Profundus (MAMPP)

The MAMPP is medial to the MAMPS. It originates from the medial edge of the quadrate and inserts into the medial crest of the compound bone (Figure 11).

The MAMPS and MAMPP do not show variation between the studied species.

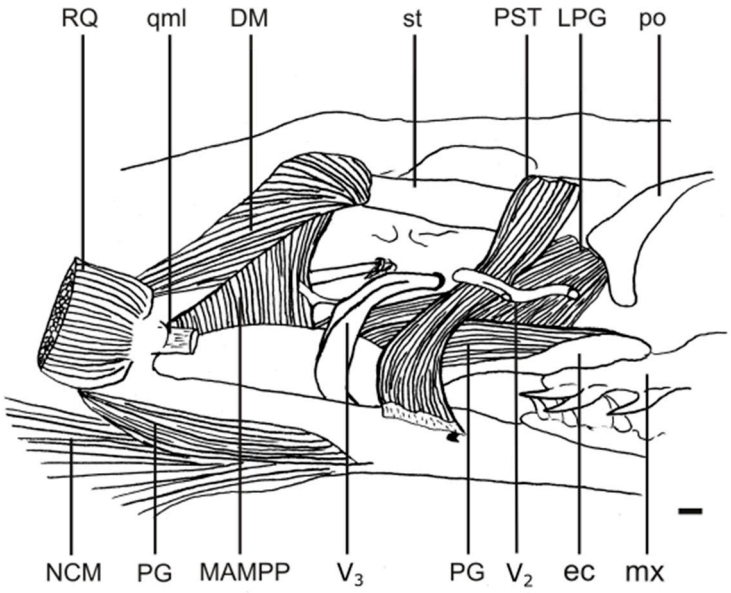

Figure 11. Jaw musculature of *Elaphe schrenckii* after removing M. adductor mandibulae externus medialis (MAMEM) and M. adductor mandibulae posteriori superficialis (MAMPS).

3.2.6. Musculus Pesudotemporalis (PST)

A thin and delicate muscle, PST is superficially covered by MAMEM and the LAO and passes under the maxillary branch of the trigeminal nerve (Figure 11). It originates ventrally from the rostral edge of the supratemporal and parietal bones to the crista parietalis. The fibres pass ventrally and slightly, caudally parallel to the anterior edge of the MAMEM. It inserts medially into the anterior insertion of the MAMEM. The origin of this muscle is on the crista temporalis or below (see Figure 12).

In all of the studied species, with the exception of *Gonyosoma oxycephalum*, this muscle originates on the parietal bone between the postorbital and supratemporal bones. In *Gonyosoma*, it reaches the postorbital bone.

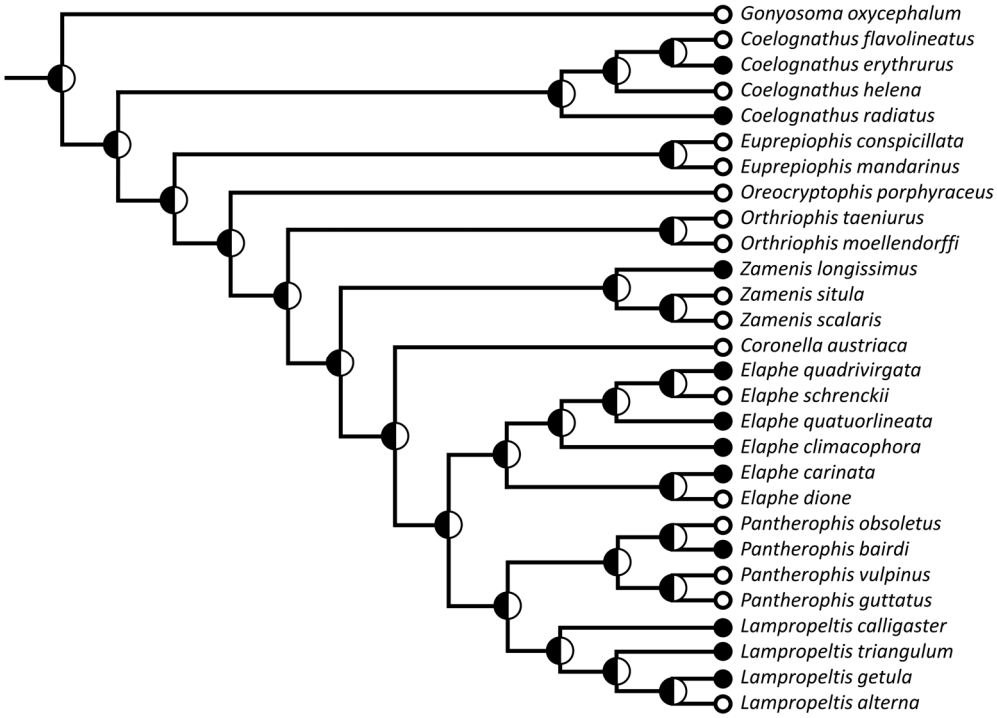

Figure 12. Variation in character states and reconstructed ancestral states of M. pseudotemporalis (PST) (M7); the cranial origin is located on the crista temporalis (white), ventral to the crista temporalis (black). Proportional likelihoods for ancestral states are given in Supplementary File S1.

3.2.7. Musculus Pterygoideus (PG)

The PG is among the biggest jaw adductor muscles in snakes. It originates on the lateral, ventral, and partially medial parts of the compound bone, around the mandibular fossa and caudal to the retroarticular process of the dorsal surface of the ectopterygoid, where it inserts via a strong tendon. This muscle does not show variation between the studied species.

3.3. Dorsal Constrictors

3.3.1. Musculus Levator Pterygoidei (LPG)

The LPG is a large, cone-shaped muscle originating from the lateral wall of the parietal bone, between the anterior-most edge of the supratemporal bone and posterior to the postorbital–parietal suture (Figures 11 and 13C). Its fibres pass caudo-ventrally down to the pterygoid. The insertion of this muscle, together with the insertion of PP, almost entirely covers the dorsal surface of the pterygoid. It reaches from the palato–pterygoid articulation and passes caudally through approximately half of the pterygoid length, also covering part of the ectopterygoid (Figure 9, Figure 11, Figure 13C,D, Figures 14 and 15).

Its cranial origin does not show significant variation. However, the pterygoid insertion of this muscle is much more variable (Figure 15, M8). In *Coelognathus helena*, it covers almost three quarters of the pterygoid surface area, whereas, in *Euprepiophis conspicillata* and *Elaphe climacophora*, it is largely reduced and covers one quarter of the pterygoid surface area.

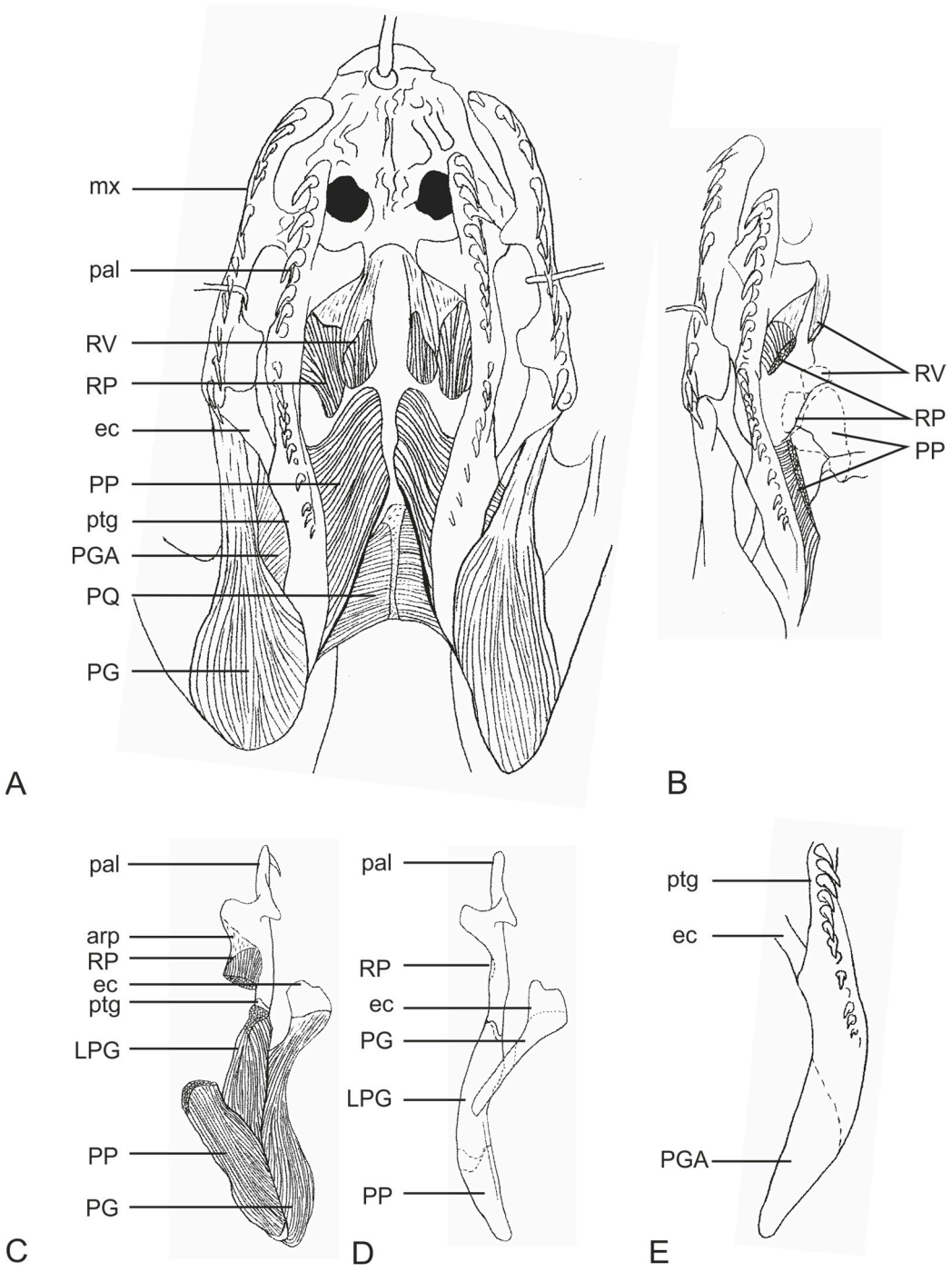

Figure 13. Dorsal constrictors of *Elaphe schrenckii*. (**A**) Ventral view after removing connective tissues, (**B**) cranial insertions of dorsal constrictors in ventral view, (**C**) dorsal view on palatine, pterygoid, and ectopterygoid and their musculature, (**D**) muscle insertions into palatine, pterygoid, and ectopterygoid in dorsal view, and (**E**) insertion of M. pterygoideus accessorius (PGA) into pterygoid in ventral view.

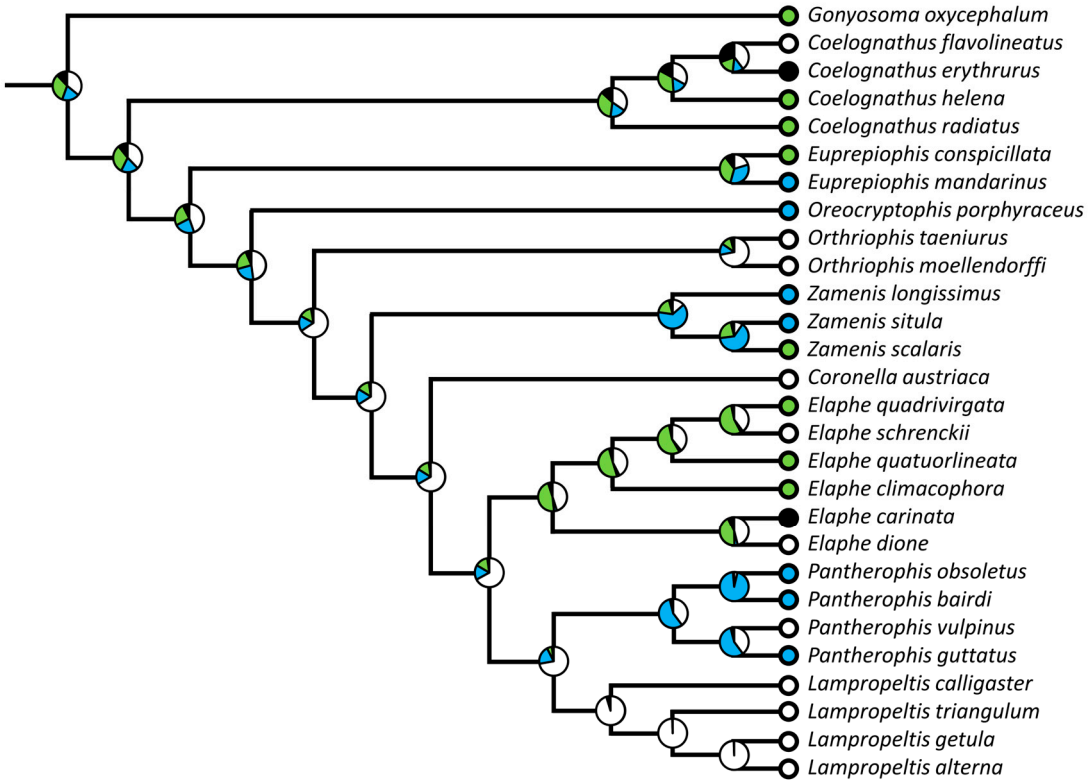

Figure 14. Variation in character states and reconstructed ancestral states of M. Levator pterygoidei (LPG) (M8); the caudal insertion is medium-sized (white), reduced anteromedially (blue), strongly reduced (green), highly elongated, and covers approximately 75% of the bone (black). Proportional likelihoods for ancestral states are given in Supplementary File S1.

3.3.2. Musculus Protractor Pterygoidei (PP)

The PP, a large muscle, originates on the caudal edge of the pterygoid crest on the basisphenoid, and its insertion passes caudally until the edge of the basioccipital crest and laterally on the prootic. Its fibres pass caudally, laterally, and ventrally through the dorsal surface of the pterygoid, caudal to the LPG insertion (Figure 13C,D).

This muscle is variable in the shapes of both its cranial origin and pterygoid insertion (Figures 15–17). In most species, the PP insertion covers approximately one third of the pterygoid surface. In most cases, its medial edge is more elongated than its lateral one, with the exception of *Oreocryptophis porphyraceus* and *Euprepiophis mandarinus*, in which the lateral edge is longer. The greatest surface of the muscle insertion is observed in *Euprepiophis conspicillata* and *Elaphe climacophora* (approx. 2/3 of the surface). In *Coelognathus erythrurus* and *Elaphe carinata*, its surface is significantly reduced (1/4). The cranial insertion may only be on the basisphenoid, with different degrees of the reduction (Figures 16 and 17). In *Coronella austriaca*, *Elaphe quadrivirgata*, and *El. schrenckii*, it reaches as far as the basioccipital. Moreover, it may be wide, laterally reaching the prootic (*El. schrenckii*), or thin (*El. quadrivirgata*) (Figure 16).

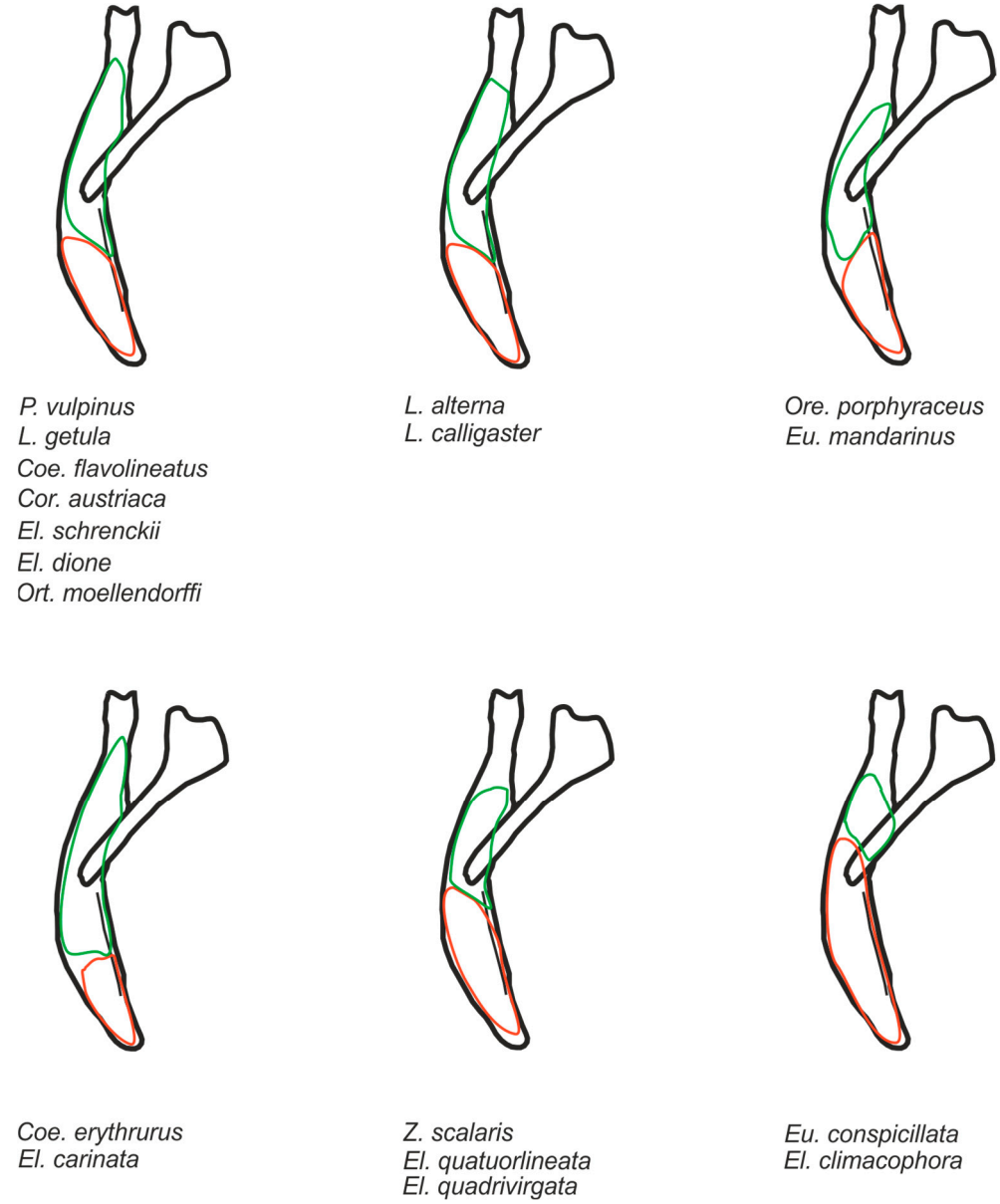

Figure 15. Schematic representation of variation in M. protractor pterygoidei (PP) (orange) and M. levator pterygoidei (green) on the left pterygoid, palatine, and ectopterygoid. The muscles are outlined on the skull of *Elaphe schrenckii*.

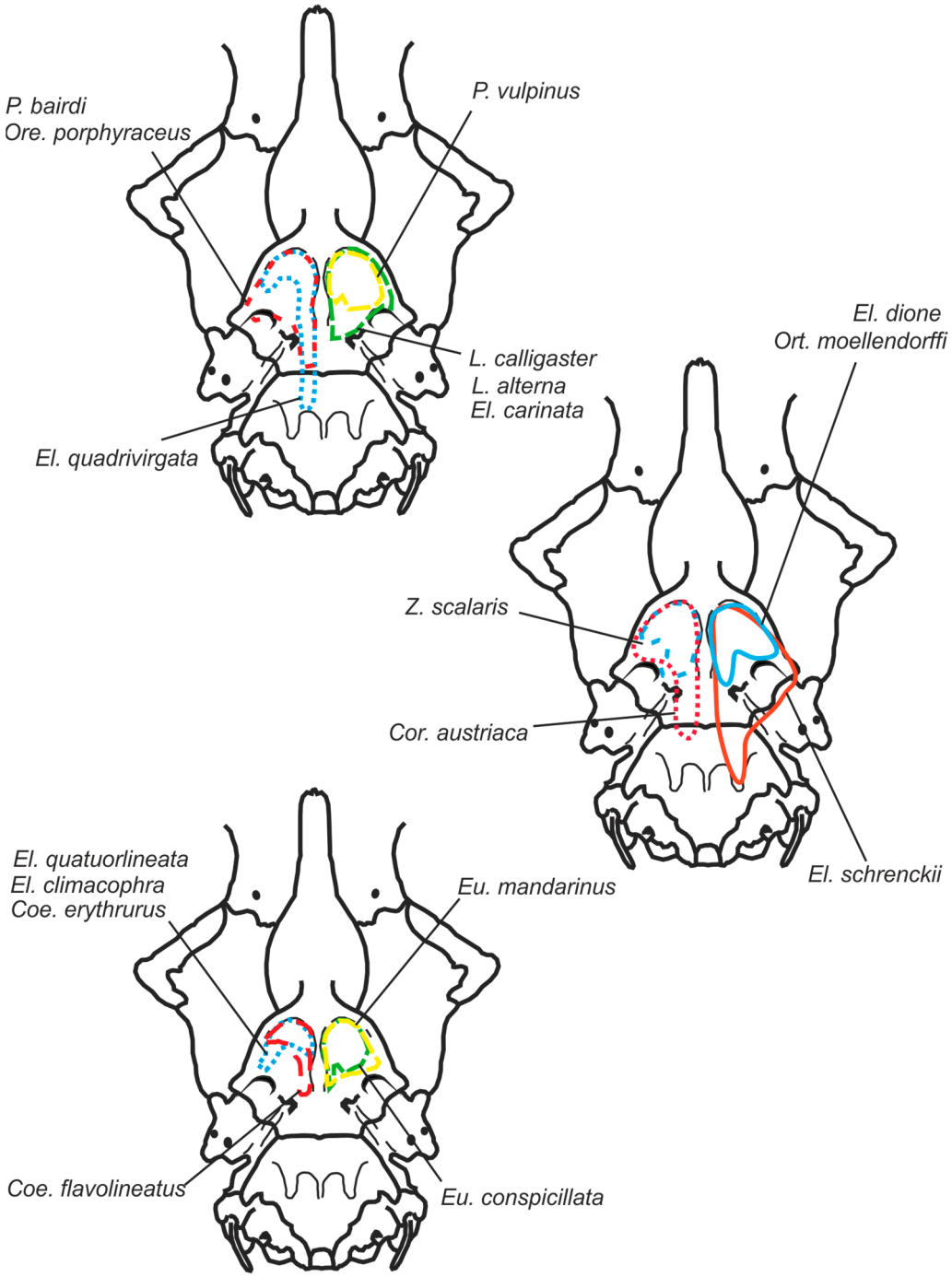

Figure 16. Schematic representation of variability in cranial insertions of M. protractor pterygoidei (PP) on skull base. The muscles are outlined on the skull of *Elaphe schrenckii*.

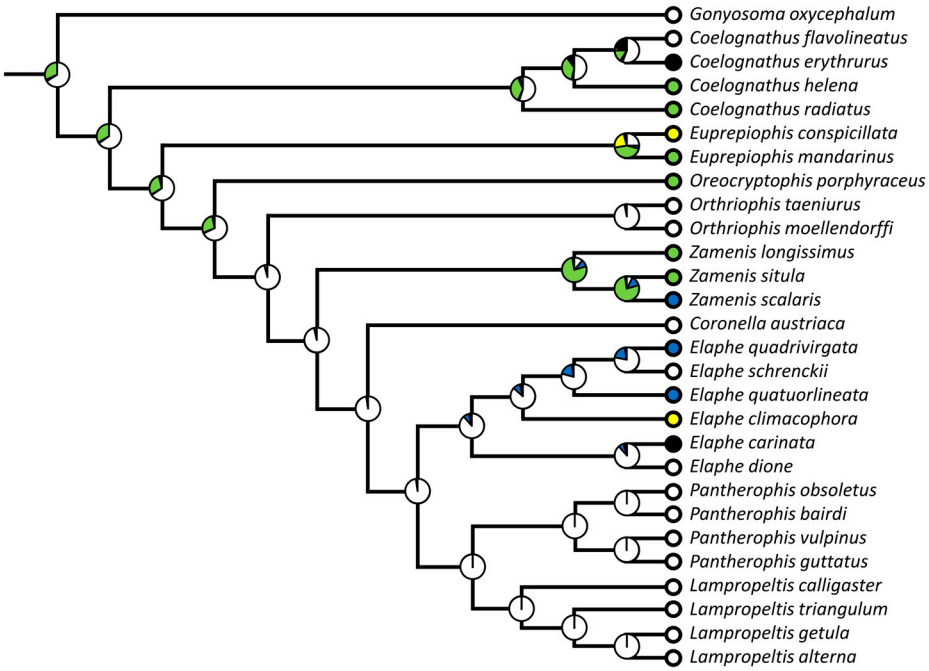

Figure 17. Variation in character states and reconstructed ancestral states of M. protractor pterygoidei (PP) (M9); the attachment to the pterygoid is medium-sized, slightly elongated along the medial margin (white), slightly enlarged, elongated along the medial margin (blue), medium-sized, elongated along the lateral margin (green), large and well-developed (yellow), and small and reduced (black). Proportional likelihoods for ancestral states are given in Supplementary File S1.

The shapes of the cranial origin of the PP in *Pantherophis bairdi*, *Oreocryptophis porphyraceus*, and *Coronella austriaca* are very similar. In *Elaphe carinata*, *Lampropeltis alterna*, and *L. calligaster*, the origin is reduced in its caudal portion. In *Elaphe* (except *El. schrenckii* and *El. quadrivirgata*), *Orthriophis*, *Zamenis scalaris*, and *Coelognathus erythrurus*, the insertion shape resembles a reversed letter U. In *Z. scalaris* and *Elaphe dione*, it is quite broad, whereas in *El. climacophora*, *El. quatuorlineata*, and *Coe. erythrurus*, it is much more narrow with a partially reduced medial area. *Coelognathus flavolineatus* also possesses a U-shaped PP insertion, however, with a reduced lateral portion and a caudally elongated medial part. Both *Euprepiophis* species are rather short, but wide, and triangular in shape and have cranial origins and relatively large surfaces (Figures 16 and 18).

3.3.3. Musculus Retractor Pterygoidei (RP)

The RP is a rather short muscle. Its cross section is oval and becomes flat in the rostral part of the muscle. Its cranial insertion is located on the rostral edge of the basisphenoid and partially at the ventral parts of the parietal. It spreads rostrally and some of its fibres insert directly into the palatine, whereas its medial part inserts via a short aponeurosis into the vomerine process (Figure 13A–C).

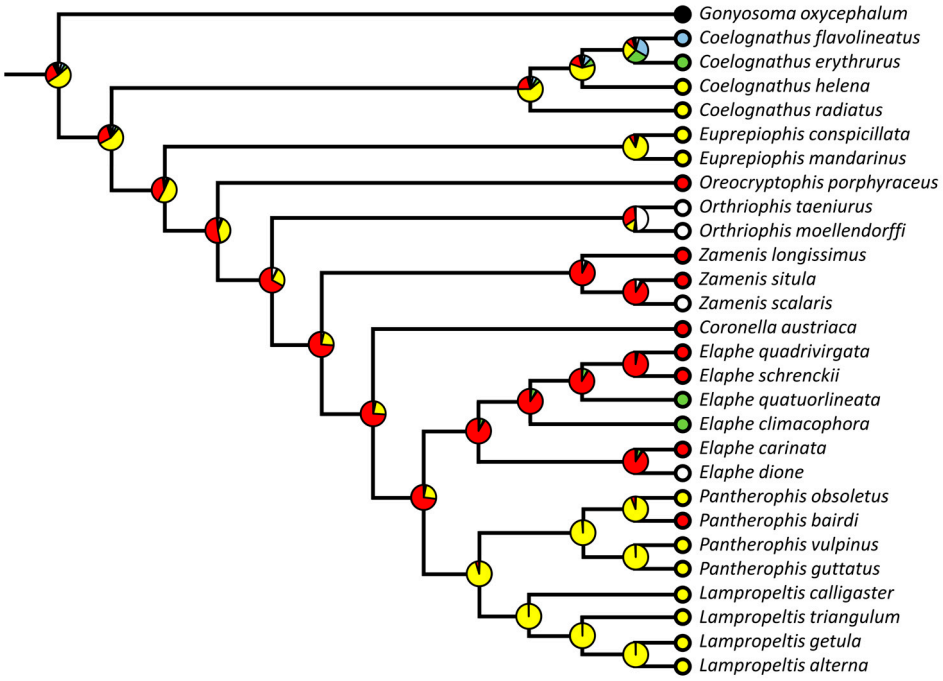

Figure 18. Variation in character states and reconstructed ancestral states of M. protractor pterygoidei (PP) (M10); the cranial origin is U-shaped (white), medial branch is slightly elongated (light blue), lateral branch is slightly elongated (green) or triangular (yellow), lateral branch is strongly elongated (red), medial branch is strongly elongated (black). Proportional likelihoods for ancestral states are given in Supplementary File S1.

There is a noteworthy variation in this muscle. Two species, *Gonyosoma oxycephalum* and *Coelognathus flavolineatus*, have a peculiar type of RP distal insertion. In these species, the RP inserts into the palatine and via the broad aponeurosis with the prefrontal bone. In *Gonyosoma*, the RP inserts directly into the palatine, and the aponeurosis reaches the prefrontal bone (Figures 19 and 20); in *Coe. flavolineatus*, it inserts via the aponeurosis, both into the palatine and prefrontal bones. It also shows variation in its size and shape of origin, which may be small and oval shaped or large and elongated (Figure 21).

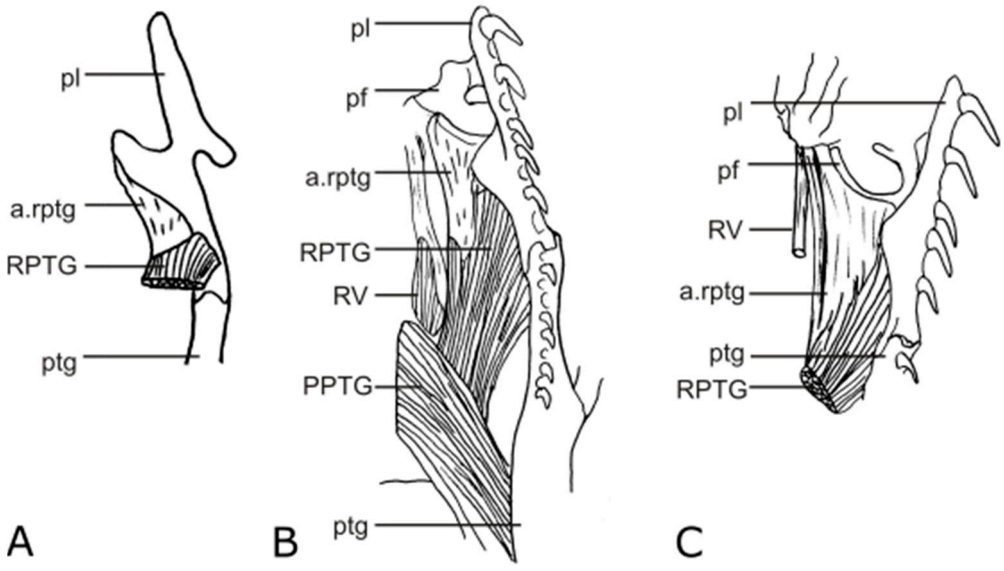

Figure 19. Distal insertions of M. retractor pterygoidei (RP) into *Lampropeltis triangulum* (**A**) and *Gonyosoma oxycephalum* (**B**,**C**). (**A**) Dorsal view, (**B**) ventral view, and (**C**) ventro-medial view.

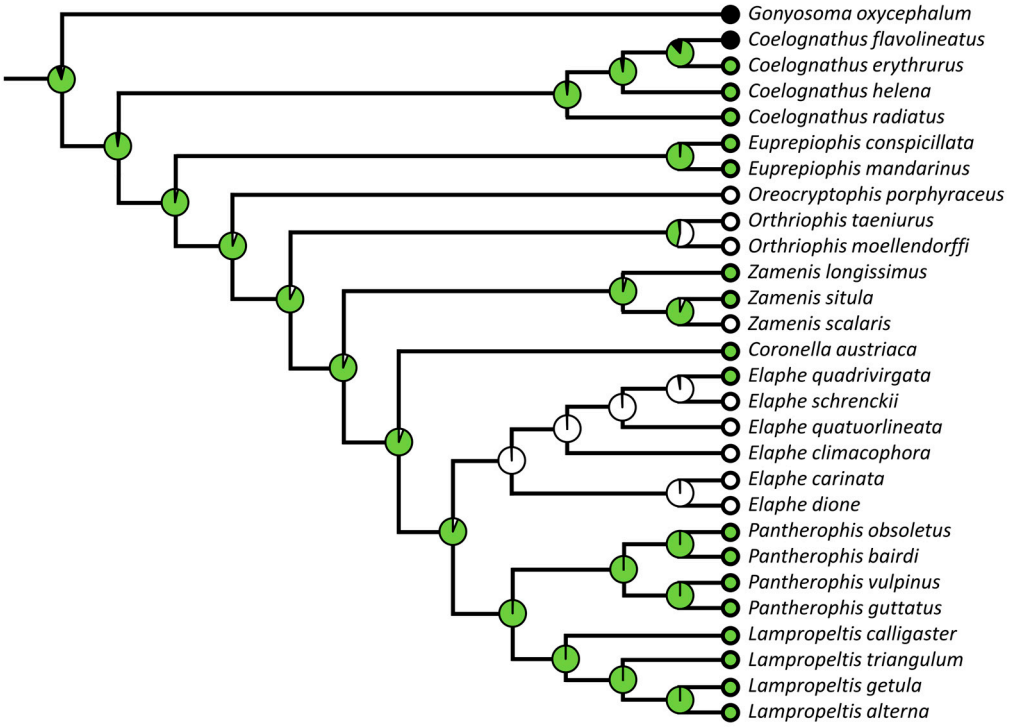

Figure 20. Variation in character states and reconstructed ancestral states of M. retractor pterygoidei (RP) (M11); the caudal insertion (aponeurosis) is reduced (white), well developed (green), or reaches the postorbital (black). Proportional likelihoods for ancestral states are given in Supplementary File S1.

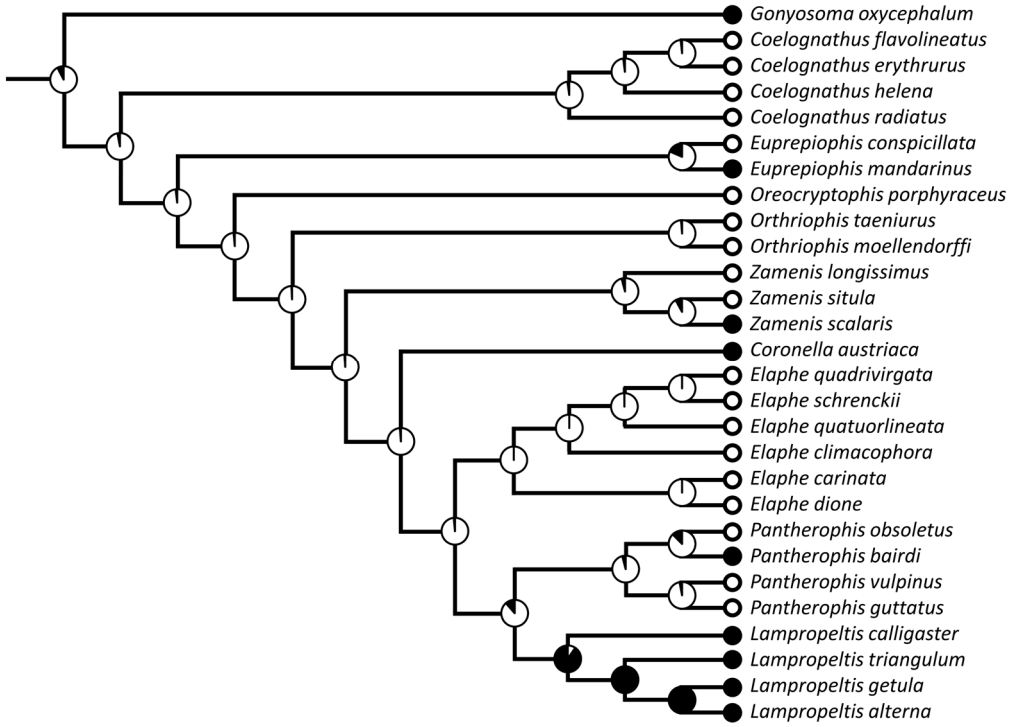

Figure 21. Variation in character states and reconstructed ancestral states of M. retractor pterygoidei (RP) (M12); the cranial origin is small and oval (white) or large and elongate (black). Proportional likelihoods for ancestral states are given in Supplementary File S1.

3.3.4. Musculus Retractor Vomeris (RV)

The RV is a small muscle, round in its cross section. Its cranial insertions are on the rostral edge of the basisphenoid crest, medial to the insertion of the RP. The medial fibres of RV are longer than its lateral ones, and this muscle rostrally contacts the posterior inferior process of the vomer via a flat, thin tendon (Figure 13A,B). Variation in the size of the origin of this muscle within the studied species was observed (Figure 22). Additionally, the aponeurosis may be strongly reduced or well developed (Figure 23).

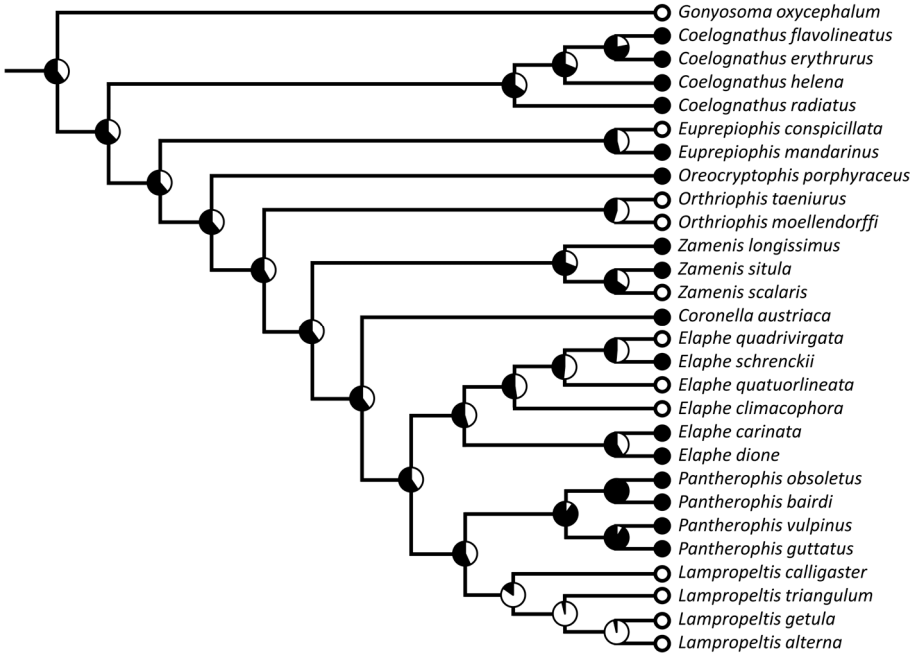

Figure 22. Variation in character states and reconstructed ancestral states of M. retractor vomeris (RV) (M13); the cranial origin is small and reduced (white) or large (black). Proportional likelihoods for ancestral states are given in Supplementary File S1.

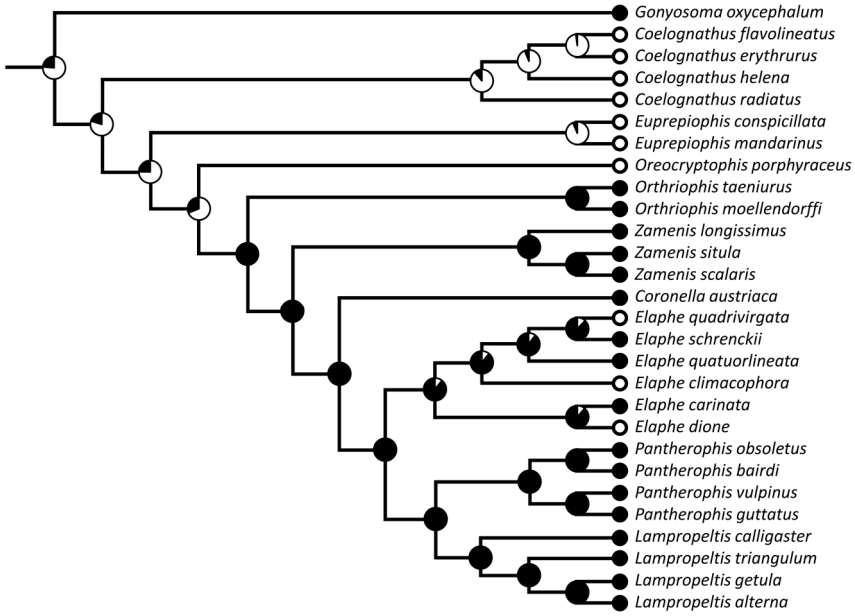

Figure 23. Variation in character states and reconstructed ancestral states of M. retractor vomeris (RV) (M14); the aponeurosis is reduced (white) or large (black). Proportional likelihoods for ancestral states are given in Supplementary File S1.

3.3.5. Musculus Protractor Quadrati (PQ)

The PQ is a thin layer of fibres located at the caudal end of the braincase, dorsal to the PGA and PP. It resembles a flat, broad triangle. The right and left PQs connect to each other via a thin connective tissue. This connective tissue in the rostral part inserts into the basioccipital, and the remaining part of the PQ is loosely connected to the membranes covering the axial musculature. Only a small portion of this muscle inserts into the quadrate. The main surfaces to which PQ attaches are the joint capsule and compound bone above the insertion of the M. pterygoideus accesorius (Figure 13A).

3.4. Intermandibular Musculature

3.4.1. Musculus Intermandibularis Anterior (MIA)

The MIA is the most rostral of the intermandibular muscles. It divides into three parts: pars anterior, p. posterior, and p. glandularis (Figure 24). Its distal insertion is on the medial wall of the dentary in its rostral part. Fibres that belong to the pars anterior pass from the most rostral part of the dentary in the medio-caudal direction and insert into the intermandibular pad. Behind them is the pars posterior of the IA. Its fibres are longer and more caudally oriented. They also insert into the intermandibular pad, but the most caudal fibres connect with the most rostral fibres of the M. intermandibularis posterior, pars anterior. The pars glandularis of the IA is strongly reduced (in *El. schrenckii*) and passes from the dorso-lateral surface of the intermandibular pad to the medio-rostral part of the lateral sublingual gland (glandula sublingualis lateralis). However, these fibres are short and not numerous.

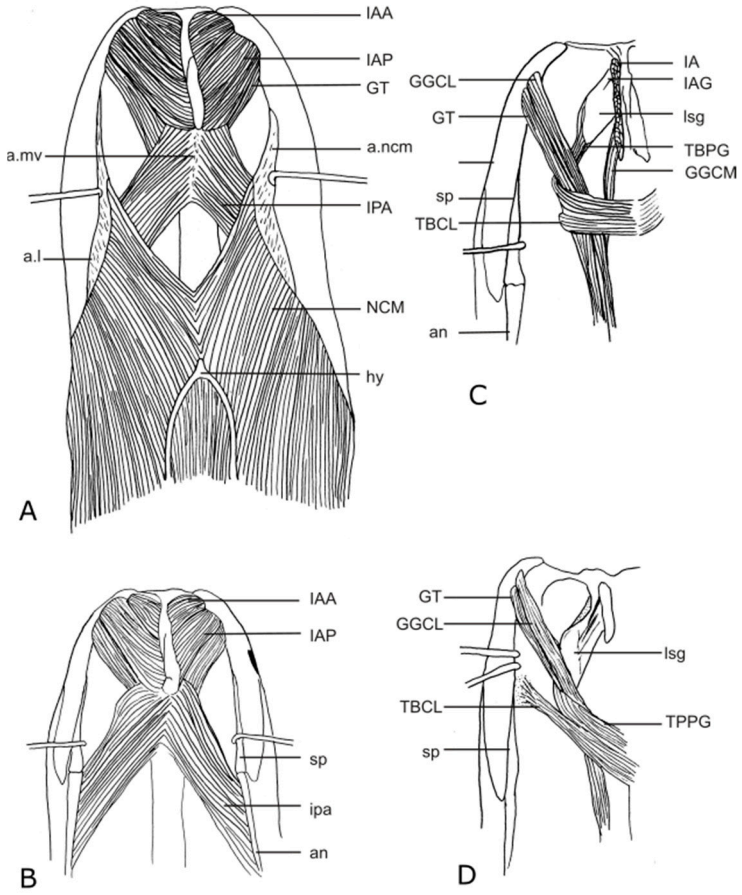

Figure 24. Intermandibular musculature of *Elaphe schrenckii* (**A**–**C**) and *Pantherophis vulpinus* (**D**) in ventral view. (**A**) Skin removed, (**B**) M. neurocostomandibularis (NCM) removed, (**C**,**D**) M. intermadibularis anterior, pars anterior et posterior (IAA and IAP), and M. intermandibularis posterior, pars anterior (IPA) removed.

3.4.2. Musculus Intermandibularis Posterior (IP)

The IP divides into two parts: pars anterior and p. posterior. The pars anterior is ventral to the pars posteriori and dorsal to the neuro-costo-mandibularis (Figure 24A,B). Its mandibular insertions are on the medial walls of the compound bone, are angular, and reach caudally as far as three quarters of the length of the angular. Its fibres are long and pass medio-rostrally. The left and right muscles connect in the medial line via a thin aponeurosis (aponeurosis medioventralis) and the most rostral fibres insert into the caudal end of the intermandibular pad and into the surface of the IMA, pars posterior.

The pars posteriori of the IP is under the skin; in the caudal end, it is also covered by M. constrictor colli. It is a very thin layer of fibres, which are easy to destroy during preparation. It inserts into the ventro-lateral walls of the compound bone and passes medially and rostrally. The most rostral fibres do not reach the caudal fibres of the pars anterior (Figure 24C).

3.4.3. Musculus Transversus Branchialis (TB)

Musculus transversus branchialis is a small, flat muscle. Its medial insertion is located over the caudal part of the IA and the most rostral part of the IP. It passes perpendicularly to the body axis under the M. genioglossus and M. geniotrachealis, then divides into two parts: the shorter one (caput laterale) passes laterally and inserts into the connective tissue of the mouth cavity, and the second part turns rostrally over the lateral caput of the genioglossus and M. geniotrachealis and inserts into the caudal part of the lateral sublingual gland (Figure 24C).

3.4.4. Musculus Geniotrachealis (GT)

The GT is a thin bundle of fibres (Figure 24C). It originates on the trachea, caudal to the intramandibular joint. It is oriented rostrally, parallel to the genioglossus, and passes under the loop of the medial caput of TB. Next, the fibres turn laterally and, together with the lateral part of the genioglossus, insert into the medial wall of the dentary.

3.4.5. Musculus Genioglossus (GG)

The GG consists of two thin bundles, first one parallel to the trachea and the second one to the GT (Figure 24C). The GG inserts into the lateral wall of the tongue pocket, and this insertion reaches caudally behind the caudal end of the braincase. Rostrally, the GG divides into two separate bundles. The medial part (caput mediale) inserts into the caudal portion of the intermandibular pad, over the caudal fibres of the IA. The lateral part of the GG (caput laterale) turns parallel with the GT just behind the TB loop. The lateral caput of the GG inserts into the dentary, rostro-ventral to the GT insertion.

The only muscle of the intermandibular series that showed variation is the TB. This muscle differs in the position of the insertion of its lateral part. In most of the studied species, it inserts into the connective tissue of the mouth cavity. The exception is *Pantherophis vulpinus*; in this species, this insertion is very close to the dentary, on the border of the connective tissues of the mouth cavity and those surrounding the bone (Figure 24D).

4. Discussion

The development of muscles (and soft tissues in general) strongly affects bone morphology (e.g., [42]; the so called 'morphogenetic primacy' of Witmer [43]). However, myology is not always a perfect representation of osteology (e.g., this work and [24]).

Radovanović [33] described the quadrate-maxillary ligament in *Elaphe quatuorlineata* and *Zamenis longissimus* as attaching to the skin near the corner of the mouth, whereas, in *Z. situla*, it is divided and inserts into the skin and maxilla. This description is erroneous, since the quadrate-maxillary ligament in all studied specimens (including members of the three species studied by Radovanović [33]) attaches directly to the rostral maxilla and is not divided on the bone and skin attachments. Probably, tight connective tissues in this area may have caused a mistake in interpretation. Radovanović [33] reported on a lack of

the PST (referred by him as M. temporalis anterior) in *Z. longissimus*. However, this muscle, although thin and delicate (and thus easy to accidentally destroy), is present in all studied species, including the Aesculapian snake.

The division of the MAMP into two parts, namely the superficialis and profundus, was criticised by Young [44]. Young argued that the crista medialis divides the distal insertion into two parts, which wrongly suggests the division of this muscle. However, although the fibres of the pars superficialis and pars profunda are in the same direction and topographically very close, these layers are separate. The proximal insertion of the pars superficialis is on the ventral surface of the crista quadrati, under the MAMES insertion. In the species in which the crista quadrati is not on the most ventro-rostral edge of the quadrate, the bone crest separates the muscle layers that insert into the fossa mandibularis (namely the MAMPS) from those inserting on the medial wall of the crista medialis (the MAMPP). Fibres referred to as the MAMPP insert into the rostral and medial surfaces of the quadrate. These two layers, although tightly adhered, are separate. However, it must be stressed that, because of their topographical similarity, tight adhesion, and similar function and direction, the fusion and/or origin of an interconnection is possible in some species, as has been described in birds [45].

Zaher [16] suggested that the presence of a strongly developed basal aponeurosis may be a paedomorphic trait when present in adult specimens. We noticed well developed basal aponeuroses in young specimens and strongly reduced or absent aponeuroses in adult ones (except for *Pantherophis bairdi* and *P. vulpinus*, Figure 9B), and Zaher [16] reported similar observations in *Clelia clelia*, in which young specimens had better developed basal aponeuroses compared to mature snakes.

Many studies on myology are based on the dissections of single animals (e.g., [17,21]). This is due to the scarcity of specimens available for dissection [46], but also, to some extent, to the arduous process of muscle preparation and observation, which may prevent some researchers from broader sampling. Although this does not pose a problem with broad scale comparisons, such as those between families or orders, it has limitations with comparisons between more closely related species. However, in this study, up to nine specimens per species were dissected and the intraspecific variation in the better represented species was very low; namely, it seems to be indetectable using standard procedures, and similar observations have been made by Cundall [24], Varkey [23], and Weaver [22]. Although snake skull bones are much more variable in size and shape at the species level (e.g., [47]), it seems that muscles may vary independently, at least to some degree, from osteological characters, as suggested by Cundall [24]. These may be functional limitations of the snake feeding system (mobility and flexibility of gape instead of powerful bite), which restrict the origin of variation within the jaw musculature. However, because of the scarcity of data on intraspecific variation within these characteristics, conclusions may be premature and further studies are needed.

The intermandibular muscles (together with the GGCL, GGCM, and GT) did not show intra- and interspecific variation. In other colubrid species, this pattern is also very similar, and there are practically no between-species differences in Natricinae (*Nerodia* and *Thamnophis*) [21,23,44], Xenodontinae (*Heterodon* and *Xenodon*) [22], and Colubrinae (*Pantherophis*, *Entechinus*, *Opheodrys* and *Simphymus* and the species described here) [9,24]. Similarly, there was no variation within the MAMPS and MAMPP; a possible reason for this is space limitations, especially in the case of the posterior adductors (the MAMPS and MAMPP), together with functional limitations [41,45].

As this study shows, dorsal constrictors (palato-pterygoid musculature) are more variable than jaw adductors or ventral constrictors (intermandibular musculature). These muscles (jaw adductors and ventral constrictors) are under strong selective pressure to be very elastic and flexible. The palatal muscles are not under such restrictions because the movements of the palato-pterygoid bar are much more restricted compared to the mandible-quadrate complex, and their main function is prey transport when swallowing, or moving the palato-pterygoid bar forward and backward [48]. Because most of the studied species

feed on quite similar prey types [31] and represent very generalised colubrid morphology, a possible correlation with prey type may not be detectable, and, again, more studies focusing on interspecific variation and more ecological data (preferred prey type) are needed.

5. Conclusions

The jaw musculature of the studied group does not show a high level of variation. It is possible that this pattern of conservatism is universal among several colubrid lineages, and that more variation occurs at the family level. It is possible that the cephalic musculature evolved, at least in some aspects, independently to the osteological characters. However, more studies on the development and comparative anatomy of the head musculature of phylogenetically diverse lineages are needed.

Supplementary Materials: The following supporting information can be downloaded at: https://www.mdpi.com/article/10.3390/d15050628/s1, Table S1: Estimated divergence dates for given clades for the temporally calibrated ancestral state recon-structions. Numbers refer to clades shown in Figure 1. File S1: Proportional likelihoods for recon-structed ancestral states. References [34,49] are cited in the Table S1.

Author Contributions: Conceptualisation, B.B.; methodology, B.B. and T.S.; software, T.S.; validation, B.B.; formal analysis, B.B. and T.S.; investigation, B.B.; resources, B.B.; data curation, B.B. and T.S.; writing—original draft preparation, B.B.; writing—review and editing, B.B. and T.S.; visualisation, B.B. and T.S.; supervision, B.B.; project administration, B.B.; funding acquisition, B.B. All authors have read and agreed to the published version of the manuscript.

Funding: This research received no external funding.

Institutional Review Board Statement: Not applicable—the specimens used in the study come from museum collections.

Informed Consent Statement: Not applicable.

Data Availability Statement: All data generated in this study are available in this manuscript and the accompanying Supplementary Materials.

Acknowledgments: BB thanks Andrzej Witkowski and Jan Kotusz (MNHW), Alan Resetar (FMNH), Wolfgang Boehme (ZFMK), Ivan Ineich (MNHN), and Rainer Guenther (ZMB) for providing the specimens dissected in this work. We are grateful to Krister T. Smith and three anonymous reviewers for their constructive comments.

Conflicts of Interest: The authors declare no conflict of interest.

Abbreviations

The list of anatomical abbreviations used in the text is provided below:

a.l	aponeurosis lateralis
a.lao	aponeurosis M. levator anguli oris
a.mv	aponeurosis medioventralis
a.ncm	aponeurosis neurocostomandibularis
an	angular
bd	bodenaponeurosis
bo	basioccipital
bs	basisphenoid
cs	compound bone (os compositum)
DM	depressor mandibulae
dt	dentary
ec	ectopterygoid
GGCL	M. genioglossus, caput lateralis
GGCM	M. genioglossus, caput medialis
GT	M. geniotrachealis
hg	glandula Harderii

hy	hyoid
IA	M. intermandibularis anterior (pp. posterior et anterior)
IAA	M. intermandibularis anterior, pars anterior
IAG	M. intermandibularis anterior, pars glandularis
IAP	intermandibularis anterior, pars posterior
ilg	glandula infralabialis
IPA	M. intermandibularis posterior, pars anterior
IPP	M. intermandibularis posterior, pars posterior
LAO	M. levator anguli oris
LPG	M. levator pterygoidei
lsg	glandula sublingualis lateralis
MAMEM	M. adductor mandibulae externus medialis
MAMEP	M. adductor mandibulae externus profundus
MAMES	M. adductor mandibulae externus superficialis
MAMPP	M. adductor mandibulae posterior profundus
MAMPS	M. adductor mandibulae posterior superficialis
mx	maxilla
NCM	M. neurocostomandibularis
pa	parietal
pal	palatine
PG	M. pterygoideus
po	postorbital
PGA	M. pterygoideus accesorius
PP	M. protractor pterygoidei
PQ	M. protractor quadrati
pr	prootic
PST	M. pseudotemporalis
ptg	pterygoid
qa	quadrate aponeurosis
qml	ligamentum quadrato-maxillare
RP	M. retractor pterygoidei
RQ	M. retractor quadrati
RV	M. retractor vomeris
slg	glandula supralabialis
sp	splenial
st	supratemporal
TBCL	M. transversus branchialis, caput lateralis
TBPG	M. transversus branchialis, pars glandularis
V2	nervus trigeminus (ramus maxillaris)
V3	nervus trigeminus (ramus mandibularis)

The list of anatomical abbreviations used in the text is provided below:

BB	personal collection of Bartosz Borczyk
FMNH	Field Museum of Natural History, Chicago, IL, USA
IZK	Department of Evolutionary Biology and Conservation of Vertebrates, University of Wrocław, Wrocław, Poland
MNHN	Museum National d'Histoire Naturelle, Paris, France
MNHW	Museum of Natural History, University of Wrocław, Wrocław, Poland
ZFMK	Museum Koenig Bonn, Bonn, Germany
ZMB	Museum für Naturkunde, Berlin, Germany

References

1. Uetz, P.; Freed, P.; Aguilar, R.; Reyes, F.; Hošek, J. (Eds.) The Reptile Database. Available online: http://www.reptile-database.org (accessed on 28 April 2023).
2. Groombridge, B.C. Comments on the intermandibular muscles of snakes. *J. Nat. Hist.* **1979**, *13*, 477–498. [CrossRef]

3. Cundall, D. Functional Morphology. In *Snakes: Ecology and Evolutionary Biology*; Seigel, R.A., Collins, J.T., Novak, S.S., Eds.; The Blackburn Press: Caldwell, NJ, USA, 1987; pp. 106–140.
4. Greene, H.W. *Snakes: The Evolution of Mystery in Nature*; University of California Press: Berkeley, CA, USA, 1997.
5. Lee, M.S.Y.; Bell, G.L.; Caldwell, M.W. The origin of snake feeding. *Nature* **1999**, *400*, 655–659. [CrossRef]
6. Cundall, D.; Greene, H.W. Feeding in snakes. In *Feeding: Form, and Evolution in Tetrapod Vertebrates*; Schwenk, K., Ed.; Academic Press: Cambridge, MA, USA, 2000; pp. 293–333.
7. Cundall, D.; Irish, F. The snake skull. In *Biology of the Reptilia*; Gans, C., Gaunt, A.S., Adler, K., Eds.; Society for the Study of Amphibians and Reptiles: Ithaca, NY, USA, 2008; Volume 20, pp. 349–692.
8. Haas, G. Muscles of the jaws and associated structures in the Rhynchocephalia and Squamata. In *Biology of the Reptilia*; Gans, C., Parsons, T.S., Eds.; Academic Press: Cambridge, MA, USA, 1973; Volume 4, pp. 285–490.
9. Albright, G.B.; Nelson, E.M. Cranial kinetics of the generalized colubrid snake *Elaphe obsoleta quadrivittata*. I. Descriptive morphology. *J. Morphol.* **1959**, *105*, 193–239. [CrossRef] [PubMed]
10. Kardong, K.V. Morphology of the respiratory system and its musculature in different snake genera. (Part I) *Crotalus* and *Elaphe*. *Morphol. Jahrb.* **1972**, *117*, 285–302.
11. Groombridge, B.C. Variations in morphology of the superficial palate of henophidian snakes and some possible systematic implications. *J. Nat. Hist.* **1979**, *13*, 447–475. [CrossRef]
12. Kardong, K.V. Jaw musculature of the West Indian snake *Alsophis cantherigerus brooksi* (Colubridae, Reptilia). *Breviora* **1980**, *463*, 1–26.
13. Rieppel, O. The trigeminal jaw adductors of primitive snakes and their homologies with the lacertilian jaw adductors. *J. Zool.* **1980**, *190*, 447–471. [CrossRef]
14. McDowell, S.B. The architecture of the corner of the mouth of colubroid snakes. *J. Herpetol.* **1986**, *20*, 353–407. [CrossRef]
15. Cundall, D.; Rossman, D.E. Cephalic anatomy of the rare Indonesian snake *Anomochilus weberi*. *Zool. J. Linn. Soc.* **1993**, *109*, 235–273. [CrossRef]
16. Zaher, H. Comments on the evolution of the jaw adductor musculature of snakes. *Zool. J. Linn. Soc.* **1994**, *111*, 339–384. [CrossRef]
17. Das, S.; Pramanick, K. Comparative anatomy and homology of jaw adductor muscles of some South Asian colubroid snakes (Serpentes: Colubroidea). *Vertebr. Zool.* **2019**, *69*, 93–102.
18. Daza, J.D.; Diogo, R.; Johnston, P.; Abdala, V. Jaw adductor muscles across Lepidosaurs: A reappraisal. *Anat. Rec.* **2011**, *294*, 1765–1782. [CrossRef]
19. Johnston, P. Homology of the jaw muscles in lizards and snakes—A solution from a comparative gnathostome approach. *Anat. Rec.* **2014**, *297*, 574–585. [CrossRef]
20. Diogo, R.; Abdala, V. *Muscles of Vertebrates: Comparative Anatomy, Evolution, Homologies and Development*; CRC Press: Boca Raton, FL, USA, 2010.
21. Cowan, I.M.; Hick, W.B.M. A comparative study of the myology of the head region in three species of *Thamnophis* (Reptilia, Ophidia). *Trans. R. Soc. Can.* **1961**, *45*, 19–60.
22. Weaver, W.G. The cranial anatomy of the hog-nosed snakes (*Heterodon*). *Bull. Florida State Mus.* **1965**, *9*, 275–304.
23. Varkey, A. Comparative cranial myology of North American Natricinae snakes. *Milwaukee Public Mus. Publ. Biol. Geol.* **1979**, *4*, 1–70.
24. Cundall, D. Variations of the cephalic muscles in the colubrid snake genera *Entechinus*, *Opheodrys*, *Symphimus*. *J. Morphol.* **1986**, *187*, 1–21. [CrossRef] [PubMed]
25. Utiger, U.; Schatti, B.; Helfenberger, N. The Oriental Colubrinae genus *Coelognathus* Fitzinger, 1843 and classification of Old and New World racers and ratsnakes (Reptilia, Squamata, Colubridae, Colubrinae). *Russ. J. Herpetol.* **2005**, *12*, 39–60.
26. Burbrink, F.T.; Lawson, R. How and when did Old World ratsnakes disperse into New World? *Mol. Phylogenet. Evol.* **2009**, *43*, 173–189. [CrossRef] [PubMed]
27. Pyron, R.A.; Burbrink, F.T.; Wiens, J.J. A phylogeny and revised classification of Squamata, including 4161 species of lizards and snakes. *BMC Evol. Biol.* **2013**, *13*, 93. [CrossRef]
28. Chen, X.; McKelvy, A.D.; Grismer, L.L.; Matsui, M.; Nishikawa, K.; Burbrink, F.T. The phylogenetic position and taxonomic status of the Rainbow Tree Snake *Gonyophis margaritatus* (Peters, 1871) (Squamata: Colubridae). *Zootaxa* **2014**, *3881*, 532–548. [CrossRef] [PubMed]
29. Zaher, H.; Murphy, R.W.; Arredondo, J.C.; Graboski, R.; Machado-Filho, P.R.; Mahlow, K.; Montingelli, G.G.; Quadros, A.B.; Orlov, N.L.; Wilkinson, M.; et al. Large-scale molecular phylogeny, morphology, divergence-time estimation, and the fossil record of advanced caenophidian snakes (Squamata: Serpentes). *PLoS ONE* **2019**, *14*, e0216148. [CrossRef]
30. Schultz, K.-D. *A Monograph of the Colubrid Snakes of the Genus Elaphe Fitzinger*; Koeltz Scientific Books: Havlíčkův Brod, Czech Republic, 1996.
31. Pyron, R.A.; Burbrink, F.T. Body size as a primary determinant of ecomorphological diversification and the evolution of mimicry in the lampropeltinine snakes (Serpentes: Colubridae). *J. Evol. Biol.* **2009**, *22*, 2057–2067. [CrossRef]
32. Albright, G.B.; Nelson, E.M. Cranial kinetics of generalized colubrid snake *Elaphe obsoleta quadrivittata*. II. Functional morphology. *J. Morphol.* **1959**, *105*, 241–291. [CrossRef] [PubMed]
33. Radovanović, M. Anatomische Studien am Schlangenkopf. *Jena. Z. Naturwiss.* **1935**, *71*, 179–312.
34. Kumar, S.; Stecher, G.; Suleski, M.; Hedges, S.B. TimeTree: A resource for timelines, timetrees, and divergence dates. *Mol. Biol. Evol.* **2017**, *34*, 1812–1819. [CrossRef]
35. Bock, W.; Shear, C.R. A staining method for gross dissection of vertebrate muscles. *Anat. Anz.* **1972**, *130*, 222–227.

36. Oliveira, L.D.; Grazziotin, F.G.; Sánchez-Martínez, P.M.; Sasa, M.; Flores-Villela, O.; Prudente, A.L.D.C.; Zaher, H. Phylogenetic and morphological evidence reveals the association between diet and the evolution of the venom delivery system in Neotropical goo-eating snakes. *Syst. Biodivers.* **2023**, *21*, 2153944. [CrossRef]
37. R Core Team. *R: A Language and Environment for Statistical Computing*; R Foundation for Statistical Computing: Vienna, Austria, 2023; Available online: https://www.R-project.org/ (accessed on 28 April 2023).
38. Paradis, E.; Schliep, K. ape 5.0: An environment for modern phylogenetics and evolutionary analyses in R. *Bioinformatics* **2019**, *35*, 526–528. [CrossRef] [PubMed]
39. Borges, R.; Machado, J.P.; Gomes, C.; Rocha, A.P.; Antunes, A. Measuring phylogenetic signal between categorical traits and phylogenies. *Bioinformatics* **2019**, *35*, 1862–1869. [CrossRef]
40. Maddison, W.P.; Maddison, D.R. Mesquite: A Modular System for Evolutionary Analysis. Version 3.61 (build 927). Available online: http://www.mesquiteproject.org (accessed on 28 April 2023).
41. Borczyk, B. The adductor mandibulae in *Elaphe* and related genera (Serpentes: Colubridae). In *Herpetologia Bonnensis II., Proceedings of the 13th Congress of the Societas Europaea Herpetologica, Bonn, Germany, 27 September–2 October 2005*; Vences, M., Köhler, J., Ziegler, T., Böhme, W., Eds.; Societas Europaea Herpetologica: Bonn, Germany, 2006; pp. 19–22.
42. Smith, K.T. The evolution of mid-latitude faunas during the Eocene: Late Eocene lizards of the Medicine Pole Hills reconsidered. *Bull. Peabody Mus. Nat. Hist.* **2011**, *52*, 3–105. [CrossRef]
43. Witmer, L.M. The Extant Phylogenetic Bracket and the importance of reconstructing soft tissue in fossils. In *Functional Morphology in Vertebrate Paleontology*; Thomason, J.J., Ed.; Cambridge University Press: Cambridge, UK, 1995; pp. 19–33.
44. Young, B.A. The anatomy of the head of the red-sided garter snake, *Thamnophis sirtalis parietalis*. Part II: Myology. *Zool. Jahrb. Abh. Anat.* **1989**, *118*, 325–354.
45. Elzanowski, A. Interconnection of muscles in the adductor mandibulae complex of birds. *Ann. Anat.* **1993**, *1975*, 29–34. [CrossRef] [PubMed]
46. Bell, C.J.; Mead, J.I. Not enough skeletons in the closet: Collection-based anatomical research in an age of conservation conscience. *Anat. Rec.* **2014**, *297*, 344–348. [CrossRef]
47. Olori, J.C.; Bell, C.J. Comparative skull morphology of uropeltid snakes (Alethinophidia: Uropeltidae) with special reference to disarticulated bone elements and variation. *PLoS ONE* **2012**, *7*, e32450. [CrossRef]
48. Cundall, D. Activity of head muscles during feeding by snakes: A comparative study. *Am. Zool.* **1983**, *23*, 383–396. [CrossRef]
49. Pyron, R.A.; Burbrink, F.T. Early origin of viviparity and multiple reversions to oviparity in squamate reptiles. *Ecol. Lett.* **2014**, *17*, 13–21. [CrossRef]